Quaternary Science Reviews 68 (2013) 216–236

Contents lists available at SciVerse ScienceDirect

Quaternary Science Reviews

journal homepage: www.elsevier.com/locate/quascirev

# Late Quaternary environmental changes in Marguerite Bay, Antarctic Peninsula, inferred from lake sediments and raised beaches

Dominic A. Hodgson [a,*,1], Stephen J. Roberts [a,1], James A. Smith [a], Elie Verleyen [b], Mieke Sterken [b], Minke Labarque [b], Koen Sabbe [b], Wim Vyverman [b], Claire S. Allen [a], Melanie J. Leng [c], Charlotte Bryant [d]

[a] NERC British Antarctic Survey, High Cross, Madingley Road, Cambridge CB3 0ET, UK
[b] Department of Biology, Section of Protistology and Aquatic Ecology, University of Ghent, Krijgslaan 281 S8, 9000 Gent, Belgium
[c] NERC Isotope Geosciences Laboratory, British Geological Survey, Keyworth, Nottingham NG12 5GG, UK
[d] NERC Radiocarbon Facility, Scottish Enterprise Technology Park, Rankine Avenue, East Kilbride, Scotland G75 OQF, UK

ARTICLE INFO

*Article history:*
Received 4 October 2012
Received in revised form
30 January 2013
Accepted 1 February 2013
Available online 27 March 2013

*Keywords:*
Antarctic Peninsula
Deglaciation
Climate change
Ice sheets
Sea level
Bird and seal occupation
Holocene

ABSTRACT

The Antarctic Peninsula is one of the fastest-warming regions on Earth, but its palaeoenvironmental history south of 63° latitude is relatively poorly documented, relying principally on the marine geological record and short ice cores. In this paper, we present evidence of late-Quaternary environmental change from the Marguerite Bay region combining data from lake sediment records on Horseshoe Island and Pourquoi-Pas Island, and raised beaches at Horseshoe Island, Pourquoi-Pas Island and Calmette Bay. Lake sediments were radiocarbon dated and analysed using a combination of sedimentological, geochemical and microfossil methods. Raised beaches were surveyed and analysed for changes in clast composition, size and roundness. Results suggest a non-erosive glacial regime could have existed on Horseshoe Island from 35,780 (38,650–33,380) or 32,910 (34,630–31,370) cal yr BP onwards. There is radiocarbon and macrofossil evidence for possible local deglaciation events at 28,830 (29,370–28,320) cal yr BP, immediately post-dating Antarctic Isotopic Maximum 4, and 21,110 (21,510–20,730 interpolated) cal yr BP coinciding with, or immediately post-dating, Antarctic Isotopic Maximum 2. The Holocene deglaciation of Horseshoe Island commenced from 10,610 (11,000–10,300) cal yr BP at the same time as the early Holocene temperature maximum recorded in Antarctic ice cores. This was followed by the onset of marine sedimentation in The Narrows, Pourquoi-Pas Island, before 8850 (8480–9260) cal yr BP. Relative sea level high stands of 40.79 m above present at Pourquoi-Pas Island and 40.55 m above present at Calmette Bay occurred sometime after 9000 cal yr BP and suggest that a thicker ice sheet, including grounded ice streams, was present in this region of the Antarctic Peninsula than that recorded at sites further north. Isolation of the Narrows Lake basin on Pourquoi-Pas Island shows relative sea level in this region had fallen rapidly to 19.41 m by 7270 (7385–7155) cal yr BP. *Chaetoceros* resting spores suggest high productivity and stratified surface waters in The Narrows after 8850 (9260–8480) cal yr BP and beach clasts provide evidence of a period of increased wave energy at approximately 8000 yr BP. Lake sediment and beach data suggest an extended period of regional warming sometime between 6200 and 2030 cal yr BP followed by the onset of Neoglacial conditions from 2630 and 2030 cal yr BP in Narrows Lake and Col Lake 1, respectively. Diatom and $\delta^{13}C$ vs C/N and macrofossil evidence suggest a potential increase in the number of birds and seals visiting the Narrows Lake catchment sometime after 2100 (2250–2000) cal yr BP, with enhanced nutrient enrichment evident after 1150 (1230–1080) cal yr BP, and particularly from c. 460 (540–380) cal yr BP. A very recent increase in *Gomphonema* species and organic carbon in the top centimetre of the Narrows Lake sediment core after c. 410 (490–320) cal yr BP, and increased sedimentation rates in the Col Lake 1 sediment core, after c. 400 (490–310) cal yr BP may be a response to the regional late-Holocene warming of the Antarctic Peninsula.



* Corresponding author. Tel.: + 44 1223 221635.
*E-mail address:* daho@bas.ac.uk (D.A. Hodgson).
[1] These authors contributed equally to this research.

0277-3791/$ – see front matter © 2013 Elsevier Ltd. All rights reserved.
http://dx.doi.org/10.1016/j.quascirev.2013.02.002

## 1. Introduction

The Antarctic Peninsula is one of the fastest-warming regions on Earth. With a rate of temperature increase of 3.7 ± 1.6 °C century$^{-1}$, it is warming at several times the global mean of 0.6 ± 0.2 °C century$^{-1}$ (Vaughan et al., 2003). This has resulted in shifts in species distributions, changes in lake ecology (Quayle et al., 2002), catastrophic disintegration of seven ice shelves (Hodgson et al., 2006; Cook and Vaughan, 2010; Hodgson, 2011) and accelerated discharge of 87% of continental glaciers (Cook et al., 2005). These processes look set to accelerate given IPCC predictions that future anthropogenic increases in greenhouse gas emissions will lead to a 1.4–5.8 °C rise in global temperatures by 2100 (IPCC, 2007), and climate modelling studies that show anthropogenic forcing of the Southern Hemisphere Annular Mode has played a key role in driving the local summer warming (Marshall et al., 2006). Warming is set to accelerate further once the buffering effect of the 'ozone hole' declines (Turner et al., 2009; Marshall et al., 2010).

Palaeoenvironmental records from this region are therefore urgently required to understand (1) the degree to which these recent changes fall outside of the range of natural variability, (2) how the ice sheets, relative sea level and ecosystems in the region have developed to their present status, and (3) how they might respond to the effects of continued increases in temperature. The key palaeoenvironmental datasets from the southern Antarctic Peninsula (South of 63° latitude) are those from ice cores, marine and lake sediments coupled with cosmogenic isotope exposure age dating of glacially-emplaced boulders and scoured bedrock, which, combined, constrain the retreat of the Last Glacial ice sheet (Bentley et al., 2006, 2009, 2011).

Ice cores from the Antarctic Peninsula have been limited in length due to the relatively rapid flow of ice from its mountainous spine (see Mosley-Thompson and Thompson, 2003, and references therein). New ice cores collected from more stable ice accumulation sites on the north-eastern Peninsula, for example at James Ross Island (64.21° S, 57.63° W) (Mulvaney et al., 2012), partially address this issue, but most ice cores from central and southern parts of the Peninsula typically span periods of only 1–2000 years. Some of these contain evidence of the rapid temperature changes seen in instrumental data over the last two decades (Thomas et al., 2009).

There is a reasonable distribution of marine sediment records from the region which document the deglaciation of the continental shelf (Ó Cofaigh et al., 2005; Kilfeather et al., 2011; Graham and Smith, 2012), bays and fjords (Taylor et al., 2001) and, in some cases changes in sea ice extent, ocean circulation, biological production and ecology (Domack, 2002; Allen et al., 2010). Some of these are reliably-dated using radiocarbon ages from discrete calcareous macrofossils whose marine reservoir effects are well-constrained by modern specimens (e.g., Domack et al., 2001; Allen et al., 2010).

On land, cosmogenic isotope exposure dating is beginning to constrain the onset of deglaciation (Bentley et al., 2006, 2011) (Fig. 1e). Epishelf lake sediments have provided records of ice shelf retreat (Bentley et al., 2005b; Hodgson et al., 2006; Smith et al., 2007a; Roberts et al., 2008), and geomorphological and palaeolimnological studies, evidence of the deglaciation and emergence of a former subglacial lake (Hodgson et al., 2009a, 2009b). However, to date, lake sediment records documenting environmental changes in the region between 63 and 70° South are limited (e.g., Wasell and Håkansson, 1992), and lake sediment proxies that reveal important information about changes in temperature (as a result of its influence on lake ice cover and within lake production), deglaciation, and sea level change (Hodgson et al., 2004; Hodgson and Smol, 2008) have been under exploited.

To address this, we present detailed multi-proxy analyses of two lake sediment cores from islands within a small archipelago in northern Marguerite Bay on the southern Antarctic Peninsula; one from a freshwater lake on Horseshoe Island and one from a coastal isolation basin on Pourquoi-Pas Island. This is supplemented by information on relative sea level change and marine conditions from surveys of raised beaches at three different locations within Marguerite Bay.

## 2. Site descriptions

All field sites are located in Marguerite Bay (68° 30′ S, 068° 30′ W), which is the most extensive embayment on the west side of the Antarctic Peninsula, bounded to the north by Adelaide Island and the Arrowsmith Peninsula and to the south by Alexander Island and George VI Sound (Fig. 1). From north to south it measures approximately 270 km and from east to west, 150 km. Outlet glaciers from the Antarctic Peninsula and Alexander Island drain into the northern, eastern and south-western parts of the bay. In the southern part of Marguerite Bay, George VI Ice Shelf, which occupies George VI Sound, discharges north into Marguerite Bay and south into the Bellingshausen Sea. The submarine Marguerite Trough, formed by the earlier grounded ice stream in this location, extends from the George VI Sound, to the edge of the continental shelf. This trough is between 50 and 80 km in width and roughly 370 km in length (Fig. 1c). It is over-deepened from approximately 500 m at the shelf edge to 1500 m in inner Marguerite Bay (Ó Cofaigh et al., 2005; Graham et al., 2011).

### 2.1. Horseshoe Island

Horseshoe Island (67° 51′ S, 67° 12′ W), one of the larger islands in northern Marguerite Bay, is situated at the entrance to Bourgeois Fjord (Fig. 1c, d). The underlying bedrock consists of foliated granitic gneisses of the Antarctic Peninsula Metamorphic Complex and undifferentiated volcanic rocks of the Antarctic Peninsula Volcanic Group (Matthews, 1983b). There are marked topographic differences between the northern part of the island which consists of low lying topography dominated by Mount Searle (537 m) and the more mountainous southern part dominated by Mt Breaker (879 m) and the Shoesmith Glacier that discharges into Gaul Cove. Between these is a narrow, largely ice-free elevated central col (Figs. 1d and 2a, b), the remnant of a major shear zone of uncertain age (Matthews, 1983b). There are four small lakes located on this central col at altitudes of between c. 80 and 140 m a.s.l. The lake studied, 'Col Lake 1' (unofficial name) (67° 49.870′ S, 67° 13.937′ W; Fig. 2b), is an elongate, shallow clear water lake, 162 m long, 64 m wide and 3.2 m deep situated at an altitude of c. 80 m above sea level.

### 2.2. Pourquoi-Pas Island

Pourquoi-Pas Island (67° 41′ S, 67° 30′ W) is a mountainous and heavily glaciated island situated to the north of Horseshoe Island (Fig. 1c). Its topography is dominated by Mt Verne 1635 m and Mt. Arronax 1540 m (Fig. 1e). The underlying bedrock consists of undifferentiated volcanic rocks of the Antarctic Peninsula Volcanic Group (Matthews, 1983a). Lower altitude ice-free areas are covered in a thick silty diamict with frost-sorted polygons, whilst bedrock is exposed on the higher ridges. Glacial striations run south-east to north-west, sub-parallel with the topographic axis of The Narrows. The study lake 'Narrows Lake' (unofficial name) is located on the north-eastern ice free coast adjacent to The Narrows (67° 36.054′ S, 67° 12.449′W) (Figs. 1e and 2c, d). The lake is 125 m long, and 6.2 m deep with a sill height of at 19.41 m above the present high water mark in The Narrows.

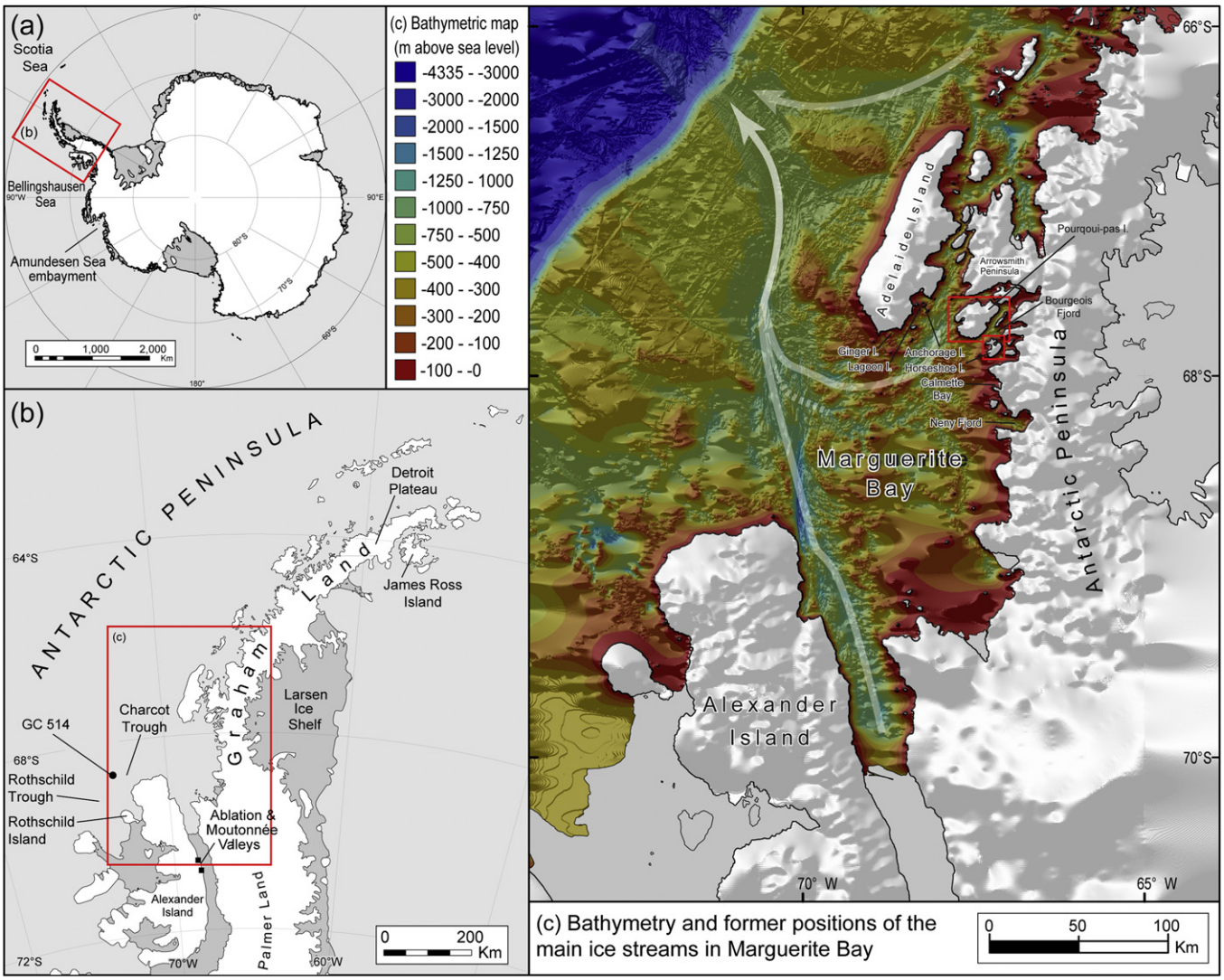


**Fig. 1.** Location maps of the Antarctic (a) Antarctic Peninsula; (b) Marguerite Bay; (c) Location of Pourquoi-Pas Island in Marguerite Bay (red boxes) and SO GLOBEC bathymetry of Marguerite Bay (from The Lamont-Doherty Earth Observatory Antarctic Multibeam Bathymetric Synthesis Database (http://data.ldeo.columbia.edu/antarctic/); (Bolmer, 2008); arrowed white lines are approximate positions of flow lines of major palaeo-ice streams which grounded on the shelf at the LGM (after, Bentley et al., 2011; Kilfeather et al., 2011; Graham and Smith, 2012; Livingstone et al., 2012); land profile is from the LIMA dataset (Bindschadler et al., 2008); (d) Horseshoe Island showing the position of Col Lake 1 and (e) Pourquoi-Pas Island showing the position of the Narrows Lake, and the transect of cosmogenic samples taken from Parvenu Point (Bentley et al., 2011). (For interpretation of the references to colour in this figure legend, the reader is referred to the web version of this article.)

### 2.3. Raised beaches

Raised beaches were first identified by aerial reconnaissance by the author and in Field Reports from early surveying expeditions, stored in the British Antarctic Survey Archives. The main raised beach sections surveyed were at Gaul Cove on Horseshoe Island (Fig. 2e; 67° 49.563′ S, 67° 12.869′ W–67° 49.613′ S, 67° 13.166′W); Pourquoi-Pas Island (Fig. 2d; c. 67° 35.52′ S, 67° 11.51′ W–c. 67° 36.02′ S, 67° 12.63′ W); and at Calmette Bay (Fig. 2f; 68° 03.848′ S, 67° 10.419 W–68° 04.040′S, 067° 10.532′ W).

## 3. Methods

### 3.1. Limnology and sediment coring

The limnology of the study sites was described following Hodgson et al. (2009b). Surface sediment cores were collected from the deepest part of the lakes using a UWITEC (1.2 m) gravity corer fitted with a steel 'orange-peel' core catcher and deeper sediments were collected with a 1 m Livingstone corer with overlaps of c. 10–15 cm between core drives. The sediment cores were unconsolidated and were therefore sectioned at 0.5 (top 20 cm) or 1 cm intervals (20 cm onwards) in the field and transported frozen in Whirlpak bags.

### 3.2. Lithology and chronology

The sediment cores were analysed for sediment colour (Troels-Smith, 1955), wet density, dry mass, and organic matter (by % weight loss on ignition (LOI), following standard methods (Dean, 1974)), and divided into stratigraphic zones.

Chronologies for the sediment cores were established by AMS radiocarbon ($^{14}$C) dating of macrofossils including microbial mats, fragments of the moss *Warnstorfia fontinaliopsis* (Muell. Hal.) Ochyra, and preserved eggs of the fairy shrimp *Branchinecta gaini* Daday, 1910. Bulk glaciolacustrine and marine sediments were dated in samples where macrofossils were absent. Paired and/or triplicate macrofossil and bulk samples were measured at selected depths in both cores to check for any systematic offsets between

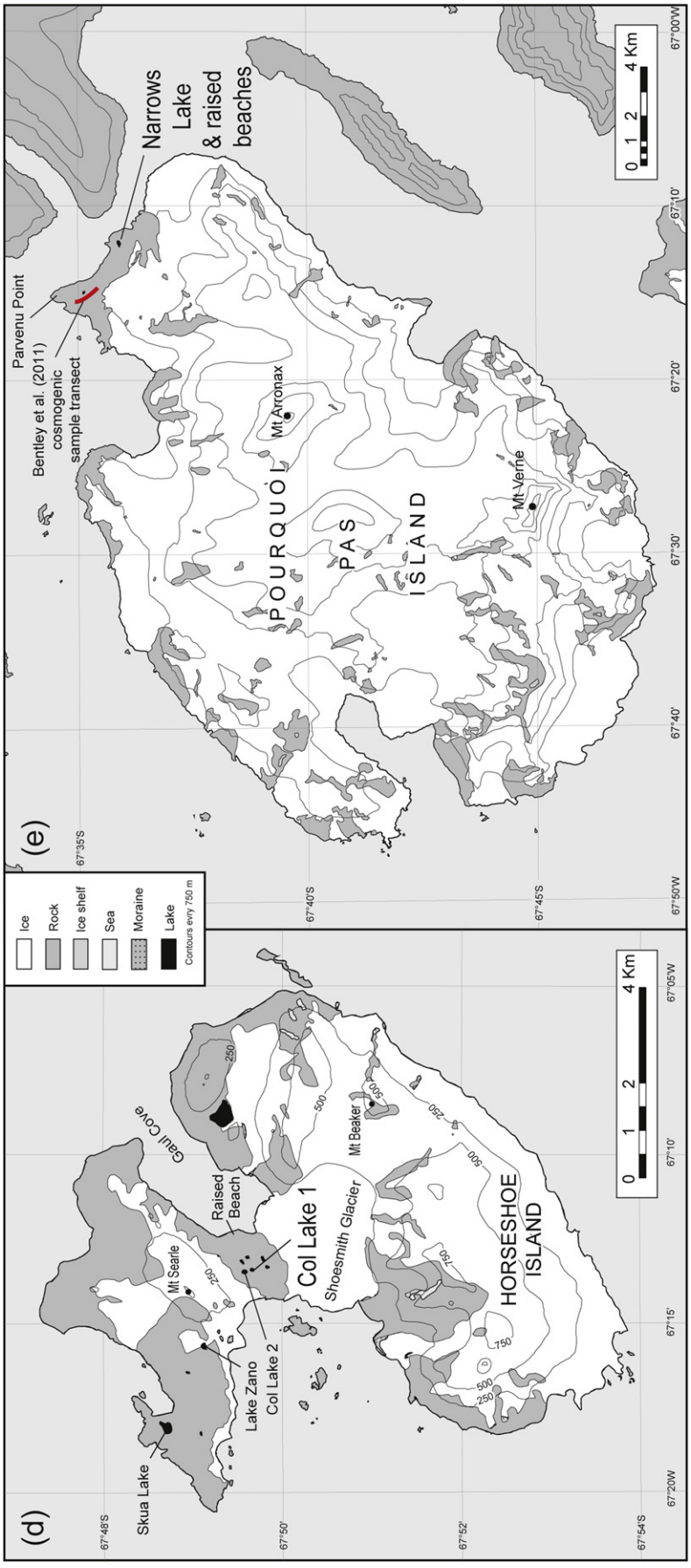


**Fig. 1.** (*continued*).

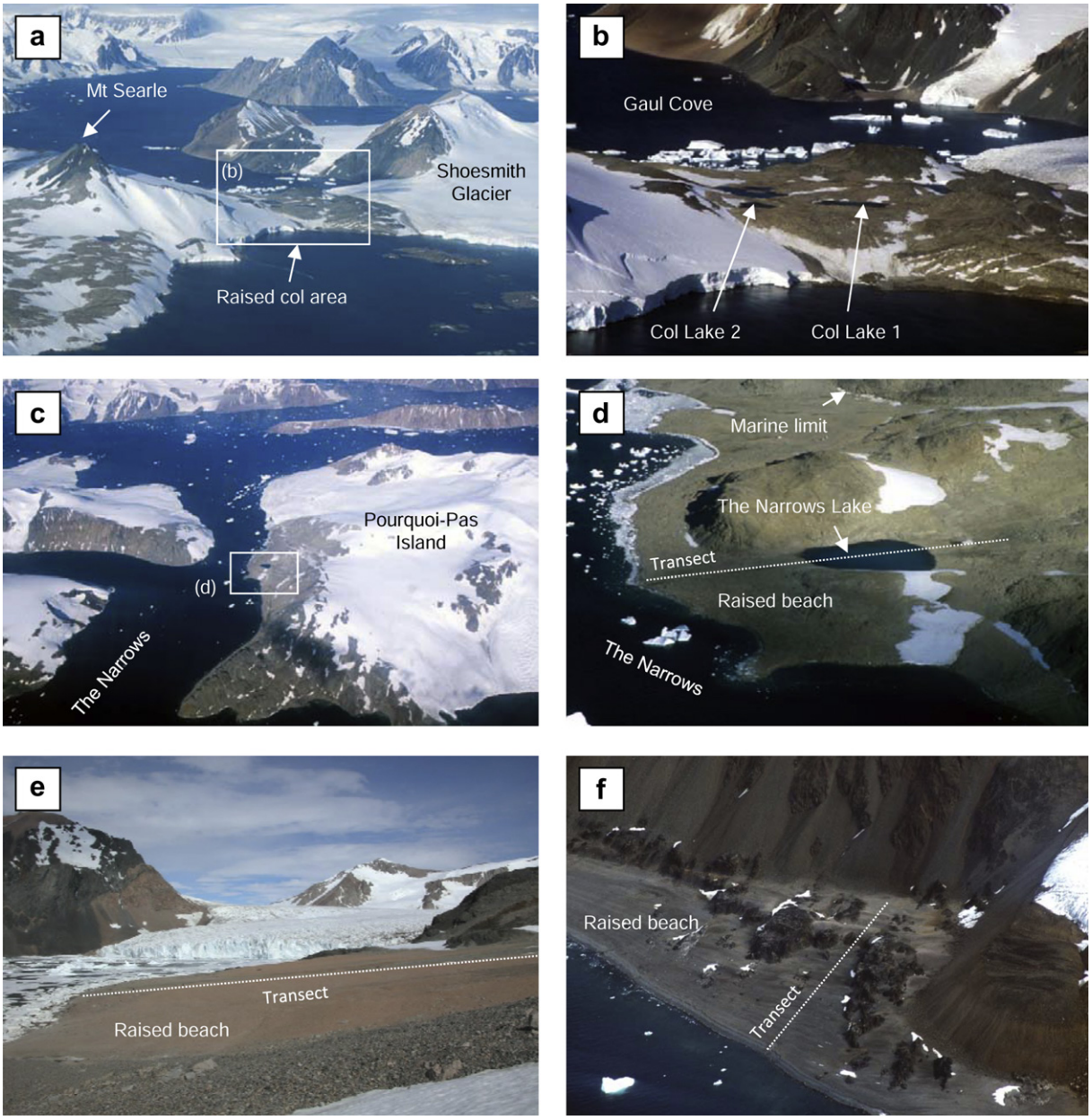


**Fig. 2.** (a) Oblique aerial view of the northern part of Horseshoe Island looking approx. east towards Mount Searle and the raised ice free col area; (b) Aerial view of the ice free col area of Horseshoe Island and Col Lake 1 looking east; (c) Aerial view of Pourquoi-Pas Island looking approx. south east along The Narrows; (d) Aerial view of the Narrows Lake showing the raised beach platform and the marine limit; (e) Raised beaches in Gaul Cove Horseshoe Island; (f) Raised beaches in Calmette Bay.

the age of the carbon incorporated in different macrofossil and bulk sediment fractions.

Macrofossils were hand-picked from frozen bulk material, after overnight defrosting at 5 °C, immersed in ultra-pure (18.2 m Ohm) water, sealed and placed in an ultrasonic bath for an hour and refrozen. Samples were sent frozen to the Scottish Universities Environmental Research Centre (SUERC) and Beta Analytic (Miami, Florida) for accelerator mass spectrometry (AMS) radiocarbon dating (Xu et al., 2004). Moss samples analysed by SUERC were soaked overnight in cold 0.5M HCl, filtered and rinsed free of mineral acid with deionised water. As samples were small, they were placed directly into quartz tubes inserts containing quartz wool and dried by freeze drying. Microbial mat samples were digested in 2M HCl (80 °C for 8 h), washed free from mineral acid with distilled water then dried and homogenised. All other SUERC-samples were heated in 2M HCl (80 °C for 8 h), rinsed in deionised water, until all traces of acid had been removed, and dried in a vacuum oven. The total carbon in a known weight of all pre-treated samples was recovered as $CO_2$ by heating with CuO in a sealed quartz tube. The $CO_2$ was converted to graphite by Fe/Zn reduction (Slota et al., 1987). Samples dated by Beta Analytic were leached with a 0.5M–1.0M HCl bath to remove carbonates, heated to 70 °C for 4 h. Leaching was repeated until no carbonate remained, followed by rinsing to neutral 20 times with deionised water, then placed in 0.5%–2% solution of NaOH for 4 h at 70 °C and rinsed to neutral 20 times with deionised water. The process was repeated until no additional reaction (typically indicated by a colour change in the NaOH liquid) was observed. Samples were then leached again in a 0.5M–1.0M HCl bath to remove any $CO_2$ absorbed from the atmosphere by the NaOH soakings and to ensure initial carbonate removal was complete, and then dried at 70 °C in a gravity oven for 8–12 h.

**Table 1**
Water chemistry of the study lakes, Col Lake 1 on Horseshoe Island and the Narrows Lake on Pourquoi-Pas Island. Additional data from nearby lakes (Col Lake 2 and a pond at Parvenu Point), and a marine sample from The Narrows are provided for comparison. Analyses followed the protocols described in Hodgson et al. (2009b).

| | | Horseshoe Island | | Pourquoi-Pas Island | | Marine |
|---|---|---|---|---|---|---|
| | | Col Lake 1 | Col Lake 2 | Narrows Lake | Parvenu Point pond | The Narrows |
| Temperature | °C | 3.7 | 5.6 | 6.4 | | 4.8 |
| Oxygen sat. | % | 96.2 | 122 | 69 | | 157.8 |
| Conductivity | µS cm$^{-1}$ | 131.2 | 166.8 | 113.2 | | 40,872 |
| ***Anions*** | | | | | | |
| Cl | mg/l | 28 | 41.4 | 34 | 29.7 | 14,700 |
| $SO_4$–S | mg/l | 13.1 | 20.1 | 11.8 | 1.3 | 664 |
| ***Cations inc. Si*** | | | | | | |
| Al | mg/l | <0.002 | <0.002 | <0.002 | 0.021 | 0.309 |
| Fe | mg/l | 0.016 | 0.003 | <0.001 | 0.002 | 0.143 |
| Mg | mg/l | 2 | 3.03 | 2.26 | 2.08 | 1050 |
| Ca | mg/l | 1.43 | 2.08 | 1.63 | 2.07 | 240 |
| K | mg/l | 0.72 | 0.894 | 0.758 | 0.768 | 330 |
| Na | mg/l | 14.6 | 21.8 | 17.2 | 16.9 | 8760 |
| Si | mg/l | 0.054 | 0.054 | 0.136 | 0.246 | 1.22 |
| ***Nutrients*** | | | | | | |
| $NO_3$–N | mg/l | <0.100 | <0.100 | <0.100 | <0.100 | <0.100 |
| $NH_4$–N | mg/l | 0.036 | 0.015 | 0.018 | 0.023 | 1.05 |
| $PO_4$–P | mg/l | <0.005 | <0.005 | <0.005 | <0.005 | 0.008 |
| ***Total N, TOC & DOC*** | | | | | | |
| DOC | mg/l | 1.06 | 0.91 | 0.58 | 0.96 | 1.51 |
| TN | mg/l | 0.14 | 0.07 | 0.04 | 0.14 | 0.14 |
| TOC | mg/l | 1.1 | 0.78 | 0.43 | 0.8 | 0.95 |

Calibration of $^{14}$C ages was carried out in OXCAL v. 4.1 (Bronk Ramsey, 2009) using the SHCal04.14C Southern Hemisphere atmosphere dataset (McCormac et al., 2004; Reimer et al., 2004) for freshwater samples. Freshwater ages older than 11,500 cal yrs BP were calibrated using the INTCAL09 Northern Hemisphere atmosphere dataset (Reimer et al., 2009). In the marine-influenced sections of the Pourquoi-Pas sediment core, a mixed MARINE09/SHCal04.14C (50% marine) (Reimer et al., 2009) calibration curve was used, and the Antarctic marine reservoir effect for this locality constrained by using a $\Delta R$ value of 664 ± 10 years (1064 ± 10 years minus the global marine reservoir of 400 years). This marine reservoir effect is based on the ages of contemporary water samples reported by Milliken et al. (2009) from Maxwell Bay (cf. Watcham et al., 2011), which has a similar coastal setting in the west Antarctic Peninsula region and is also subject to seasonal meltwater from tidewater glaciers.

Radiocarbon age data are reported as conventional radiocarbon years BP ($^{14}$C yr BP) ±1$\sigma$, and as 2-$\sigma$ (95.4%) calibrated age ranges, mean ±1$\sigma$, and median calibrated ages (cal yr BP relative to AD 1950) (Tables 2 and 3). Calibrated ages are rounded to the nearest 5 years where measured radiocarbon age errors were less than ±50 $^{14}$C years and to the nearest 10 years where measured radiocarbon age errors were greater than ±50 $^{14}$C years. Classical age–depth modelling was undertaken using CLAM v2 software (Blaauw, 2010). Interpolated ages in the text were rounded to the nearest 10 years and derived from the 'best-fit' age of the CLAM age–depth model, with interpolated 2-$\sigma$ (95%) calibrated age ranges shown in brackets, also rounded to the nearest 10 years.

### 3.3. Siliceous microfossils and macrofossils

Diatoms and stomatocysts were analysed in the Narrows Lake core, but were absent from Col Lake 1 on Horseshoe Island; a likely result of silica limitation (Table 1). Diatom preparation followed a slightly modified version of Renberg (1990). Naphrax® was used as the slide mountant. At least 400 valves and stomatocysts were counted in each sample. Taxonomy was mainly based on Sabbe et al. (2003), Van de Vijver et al. (2002) and Cremer et al. (2003). The diatom stratigraphy was divided into zones using stratigraphically constrained cluster analysis of the diatom data following squared root transformation (CONISS, Grimm, 1987). The significance of the zones was assessed using the broken stick model (Bennett, 1996) in the Rioja package for R (Juggins, 2009). Changes in the diatom communities were interpreted following previously published ecological preferences of indicator taxa.

Sediment samples for macrofossil analysis were prepared by washing bulk sediment samples (2 cm$^3$) through a 125 µm sieve using deionised water to remove fine inorganic particles. The remaining material was placed in a perspex counting chamber and macrofossils were systematically enumerated using a low-powered dissection microscope. Macrofossils included Anostracan eggs (Fairy Shrimp, *B. gaini*) and moss fragments (*Warnstorfia fontinaliopsis*, in the Narrows Lake).

### 3.4. Geochemical analyses

Geochemical analyses included measurements of total carbon (TC) and total nitrogen (TN) concentrations (%) from which C/N is derived, and bulk organic carbon isotopic ratios ($\delta^{13}C_{org}$) by combustion on a Carlo Erba 1500 on-line to a VG Triple Trap and Optima dual-inlet mass spectrometer. $\delta^{13}C_{org}$ values were calculated to the VPDB scale using a within-run laboratory standard calibrated against NBS-19 and NBS-22. Total organic carbon (TOC) and total organic nitrogen (TON) values were determined simultaneously when measuring the isotope ratio. Replicate analyses of sample material gave a precision of ±0.1 (per mil) for $\delta^{13}C_{org}$ and 10% for C/N.

### 3.5. Raised beach surveys

Raised beaches at Pourquoi-Pas Island, Horseshoe Island and at Calmette Bay (Fig. 2d–f, respectively) were surveyed up to their marine limits. Surveys were carried out using a Leica NA720 autoset level. Periods of changing coastal conditions were determined from changes in clast size and roundness (which provides an indication of past wave energy and/or sea ice cover) of raised beach material, the latter using the standard ordered scale of Powers (1953). Measurements of the *a*-axis (the longest axis of the rock) and *b*-axis (the intermediate axis, perpendicular to the *a*-axis) were also undertaken where time permitted. The beach survey and age constraint data were compared with previously published data from Ginger Islands, Lagoon Island, Anchorage Island and Rothera Point in the north and west of Marguerite Bay (Bentley et al., 2005a).

## 4. Results

### 4.1. Horseshoe Island, Col Lake 1

Being only 3.2 m deep, light penetrates to the bottom of Col Lake 1, resulting in well-developed benthic and epilithic mats of cyanobacteria, and a grazing zooplankton community including *B. gaini* and *Boeckella poppei*. Patchy moss beds are present, particularly towards the edges of the lake. The water chemistry is typical of a polar freshwater oligotrophic lake (Table 1). Profiles of the water column (measured on 17 Jan 2003) show a marginally warmer surface layer to 1.6 m followed by steady cooling through the lower water column. The water column is otherwise well mixed with little change in conductivity, and no evidence of oxygen depletion with depth (Fig. 3).

The 111 cm sediment core consisted of three lithological units (Fig. 4). The lowest unit (Lithological Unit 1, 111–72 cm) consisted of glaciolacustrine greenish grey silt with clay and sand overlain by a

**Table 2**
Radiocarbon dates for the Col Lake 1 sediment core from Horseshoe Island, including conventional $^{14}$C ages, local reservoir corrected ages, and 2-$\sigma$ calibrated age data. L-Unit is lithological unit. Calibration of $^{14}$C ages was carried out in OXCAL v. 4.1 (Bronk Ramsey, 2009) using the SHCal04. 14C atmosphere dataset (McCormac et al., 2004; Reimer et al., 2004). A Local Reservoir Correction (LRC) of 693 ± 26 $^{14}$C years was applied before calibration to sediments in Unit 3 (Model A). This LRC is based on the youngest age obtained from active microbial mats that constitute the surface sediment in this core and which should return a zero age if no in-lake reservoir effect existed. No LRC and SHCal04.14C was applied before calibration for Model B. Radiocarbon ages that extended beyond the SHCal04.14C dataset were calibrated using INTCAL09 (Model C). Absolute percentage of modern carbon (pMC) data were corrected according to $^{13}$C/$^{12}$C isotopic ratios; * indicates an estimated isotopic value where samples were too small to be measured directly; samples marked with an 'x' were considered to be reworked or outliers and not included in the age–depth modelling runs. pMC = percentage modern carbon.

| Lab ID – publication code | Core ID | Strat. depth (cm) | L-Unit | Material dated & C source | Carbon content (wt %) | $\delta^{13}C_{VPDB}$ (‰) | Measured pMC(%±1$\sigma$) | Absolute pMC (%±1$\sigma$) | Conventional $^{14}$C age (CRA) (yr BP ±1$\sigma$) | OXCAL 95.4% calibration data Curve A: LRC = 693 ± 26 $^{14}$C yrs; (cal yr BP) | | | |
|---|---|---|---|---|---|---|---|---|---|---|---|---|---|
| | | | | | | | | | | Max.–Min. | Mean ±1$\sigma$ | Median | Curve |
| ***Col Lake 1, Horseshoe Island*** | | | | | | | | | | | | | |
| SUERC-6259 | COL1-0/1U-B | 0–1 | 3.3 | Microbial mat (TOC) | 18.2 | −15.1 | 91.73 ± 0.29 | 91.14 ± 0.29 | 693 ± 26 | 55–Modern | 15 ± 20 | 10 | A |
| BETA-297498 | COL1: 0-1 | 0–1 | 3.3 | >125 μm microbial mat | – | −14.2 | 87.50 ± 0.50 | 86.89 ± 0.89 | 1070 ± 40 | 405–225 | 310 ± 45 | 310 | A |
| SUERC-5041 | COL1-2U-B | 2–3 | 3.3 | Microbial mat (TOC) | 5.9 | −12.4 | 62.90 ± 0.19 | 62.49 ± 0.19 | 3724 ± 25 | 3430–3220 | 3325 ± 50 | 3325 | A-x |
| BETA-297499 | COL1: 2-3 | 2–3 | 3.3 | >125 μm microbial mat | – | −12.6 | 64.70 ± 0.30 | 64.21 ± 0.24 | 3500 ± 30 | 3165–2930 | 3050 ± 60 | 3050 | A |
| SUERC-5042 | COL1-8.5U-B | 8.5–9 | 3.2 | Microbial mat (TOC) | 6.2 | −12.5 | 59.10 ± 0.20 | 58.71 ± 0.20 | 4225 ± 27 | 4100–3860 | 3985 ± 60 | 3985 | A |
| BETA-297500 | COL1: 8.5-9 | 8.5–9 | 3.2 | >125 μm microbial mat | – | −11.0 | 59.10 ± 0.30 | 58.63 ± 0.29 | 4230 ± 40 | 4130–3845 | 3990 ± 70 | 3990 | A |
| SUERC-5043 | COL1-24U-B | 24–25 | 3.2 | Microbial mat (TOC) | 7.2 | −11.1 | 54.19 ± 0.20 | 53.83 ± 0.20 | 4922 ± 30 | 4995–4765 | 4875 ± 55 | 4875 | A |
| SUERC-5044 | COL1-1L-B | 46–47 | 3.1 | Microbial mat (TOC) | 4.7 | −13.7 | 48.74 ± 0.21 | 48.43 ± 0.21 | 5772 ± 35 | 5945–5715 | 5830 ± 55 | 5830 | A |
| SUERC-5047 | COL1-20L-B | 65–66 | 2 | *Warnstorfia* moss | 1.0 | −15.7 | 36.04 ± 0.22 | 35.80 ± 0.22 | 8199 ± 50 | 9270–8990 | 9110 ± 80 | 9090 | B |
| SUERC-5587 | COL1-20L-E | 65–66 | 2 | *Branchinecta gaini* eggs | 12.0 | −15.3 | 35.30 ± 0.23 | 35.07 ± 0.23 | 8364 ± 51 | 9460–9130 | 9310 ± 90 | 9320 | B |
| SUERC-5585 | COL1-20L-M | 65–66 | 2 | Bulk sediment – sandy silt (TOC) | 18.8 | −15.3* | 35.85 ± 0.23 | 35.61 ± 0.23 | 8242 ± 51 | 9310–9000 | 9150 ± 90 | 9140 | B |
| SUERC-6257 | COL1-27L-B | 72–73 | 1 | Bulk sediment – silty clay (TOC) | 0.3 | −18.0* | 31.22 ± 0.23 | 31.01 ± 0.23 | 9352 ± 59 | 10,660–10,270 | 10,480 ± 100 | 10,490 | B |
| SUERC-5588 | COL1-28L-M | 73–74 | 1 | *Warnstorfia* moss | 24.3 | −17.0* | 30.88 ± 0.26 | 30.67 ± 0.26 | 9441 ± 66 | 11,000–10,300 | 10,610 ± 100 | 10,610 | B |
| SUERC-20899 | COL1-30L-B | 75–76 | 1 | Bulk sediment – silty clay (TOC) | 0.2 | −22.3 | 20.44 ± 0.13 | 20.29 ± 0.13 | 12,756 ± 53 | 15,600–14,760 | 15,170 ± 200 | 15,140 | C |
| SUERC-20900 | COL1-32L-B | 77–78 | 1 | Bulk sediment – silty clay (TOC) | 0.2 | −22.5 | 20.36 ± 0.13 | 20.22 ± 0.13 | 12,786 ± 53 | 15,660–14,880 | 15,230 ± 210 | 15,190 | C |
| SUERC-20901 | COL1-34L-B | 79–80 | 1 | Bulk sediment – silty clay (TOC) | 0.1 | −21.9 | 12.79 ± 0.12 | 12.71 ± 0.12 | 16,518 ± 77 | 20,010–19,420 | 19,670 ± 150 | 19,690 | C |
| SUERC-5048 | COL1-37L-B | 82–83 | 1 | Bulk sediment – silty clay (TOC) | 0.1 | −20.7 | 9.59 ± 0.28 | 9.53 ± 0.28 | 18,833 ± 231 | 23,330–21,850 | 22,540 ± 370 | 22,490 | C |
| SUERC-20902 | COL1-40L-B | 85–86 | 1 | Bulk sediment – silty clay (TOC) | 0.2 | −24.9* | 5.06 ± 0.12 | 5.02 ± 0.12 | 23,970 ± 193 | 29,370–28,320 | 28,830 ± 280 | 28,830 | C |
| – | COL1-40L-F | 85–86 | 1 | Organic-residue | Insufficient for $^{14}$C measurement | | | | | | | | |
| SUERC-5049 | COL1-49L-B | 94–95 | 1 | Bulk sediment – silty clay (TOC) | 0.1 | −21.2 | 2.12 ± 0.29 | 2.10 ± 0.29 | 30,964 ± 1115 | 38,650–33,380 | 35,890 ± 1300 | 35,780 | C-x |
| SUERC-5050 | COL1-65L-B | 110–111 | 1 | Bulk sediment – silty clay (TOC) | 0.1 | −21.5 * | 2.91 ± 0.29 | 2.89 ± 0.29 | 28,422 ± 807 | 34,630–31,370 | 32,970 ± 930 | 32,910 | C |

**Table 3**
Radiocarbon dates for the Narrows Lake sediment core from Pourquoi-Pas Island, including conventional $^{14}$C ages, marine reservoir corrected ages and 2-$\sigma$ calibrated age data. All symbols/abbreviations are as described in Table 2. Additionally, D-Zone is diatom zone (see Fig. 8); L or M indicates Lake (L) or Marine (M) sediment. Calibration Model D is as Model A, described in Table 2, but with a Local Reservoir Correction (LRC) of 270 ± 40 $^{14}$C yrs applied prior to calibration. In the marine-influenced sections of this core, a mixed MARINE09-SHCal04.14C (50% marine) (Reimer et al., 2009) calibration curve was used, with a $\Delta R$ value of 664 ± 10 years (1064 ± 10 years minus the global marine reservoir of 400 years) (Model E) (see text for further explanation).

| Lab ID – publication code | Core ID | Strat. depth (cm) | L-Unit | D-Zone | | Material dated & C source | Carbon content (wt %) | $\delta^{13}C_{VPDB}$ (‰) | Measured modern carbon (%±1$\sigma$) | Absolute modern carbon (%±1$\sigma$) | Conventional $^{14}$C age (yr BP ±1$\sigma$) | OXCAL 95.4% calibration data Curve D: LRC = 270 ± 40 $^{14}$C yrs; Curve E: $\Delta R$ = 664 ± 10 $^{14}$C yrs 50% marine (cal yr BP) | | | |
|---|---|---|---|---|---|---|---|---|---|---|---|---|---|---|---|
| | | | | | | | | | | | | Max.–Min. | Mean ±1$\sigma$ | Median | Model |
| ***Narrows Lake, Pourquoi-Pas Island*** | | | | | | | | | | | | | | | |
| BETA-297501 | PQP 0-1 | 0–1 | 5.5 | 4 | L | >125 μm microbial mat | – | −15.7 | 96.70 ± 0.50 | 95.98 ± 0.48 | 270 ± 40 | 120–Modern | 40 ± 40 | 35 | D |
| SUERC-5052 | PQP-0/1U-B | 0–2 | 5.5 | 4 | L | Microbial mat (TOC) | 1.0 | −18.3 | 92.07 ± 0.28 | 91.47 ± 0.28 | 663 ± 25 | 440–265 | 350 ± 45 | 355 | D |
| SUERC-5053 | PQP-9U-B | 9–10 | 5.5 | 4 | L | Microbial mat (TOC) | 1.2 | −18.5 | 85.38 ± 0.24 | 84.83 ± 0.24 | 1270 ± 22 | 955–765 | 865 ± 50 | 865 | D |
| SUERC-5720 | PQP-20U-M | 20–21 | 5.4 | 4 | L | *Warnstorfia* moss | 9.0 | −17.5* | 68.79 ± 0.33 | 68.35 ± 0.18 | 3005 ± 38 | 2980–2710 | 2840 ± 70 | 2840 | D-x |
| SUERC-5054 | PQP-21U-B | 21–22 | 5.4 | 4 | L | Microbial mat (TOC) | 2.2 | −14.7 | 72.15 ± 0.21 | 71.68 ± 0.21 | 2622 ± 24 | 2525–2270 | 2390 ± 65 | 2385 | D |
| SUERC-5589 | PQP-38U-M | 38–39 | 5.3 | 3 | L | *Warnstorfia* moss | 30.0 | −19.9 | 64.95 ± 0.22 | 64.53 ± 0.22 | 3467 ± 27 | 3530–3295 | 3410 ± 60 | 3405 | D |
| SUERC-8331 | PQP-39U-B | 39–40 | 5.3 | 3 | L | Microbial mat (TOC) | 6.9* | −14.1 | 64.02 ± 0.26 | 63.60 ± 0.26 | 3583 ± 32 | 3680–3420 | 3550 ± 65 | 3550 | D |
| SUERC-5590 | PQP-56U-M | 56–57 | 5.2 | 2 | L | *Warnstorfia* moss | 37.7 | −20.3 | 48.79 ± 0.22 | 48.47 ± 0.22 | 5765 ± 37 | 6375–6130 | 6250 ± 60 | 6250 | D |
| SUERC-5593 | PQP-56U-E | 56–57 | 5.2 | 2 | L | *Branchinecta gaini* eggs | 20.0 | −12.4 | 49.24 ± 0.22 | 48.92 ± 0.22 | 5690 ± 37 | 6290–6045 | 6170 ± 60 | 6175 | D |
| SUERC-8332 | PQP-57U-B | 57–58 | 5.2 | 2 | L | Microbial mat (TOC) | 5.5* | −14.1 | 48.79 ± 0.23 | 48.47 ± 0.23 | 5765 ± 37 | 6375–6130 | 6250 ± 60 | 6250 | D |
| BETA-180801 | PQP-11L-B | 62–63 | 5.1 | 2 | L | *Warnstorfia* moss | – | −17.4 | 44.95 ± 0.30 | 44.68 ± 0.28 | 6420 ± 50 | 7150–6840 | 7000 ± 80 | 7000 | D |
| SUERC-5059 | PQP-64U-B | 64–65 | 5.1 | 2 | L | Microbial mat (TOC) | 6.4 | −13.8 | 44.07 ± 0.21 | 43.78 ± 0.21 | 6582 ± 39 | 7280–7030 | 7160 ± 60 | 7165 | D |
| SUERC-5594 | PQP-64U-E | 64–65 | 5.1 | 2 | L | *Branchinecta gaini* eggs | 25.2 | −13.8 | 43.40 ± 0.23 | 43.12 ± 0.23 | 6705 ± 42 | 7385–7155 | 7270 ± 60 | 7270 | D |
| SUERC-5060 | PQP-70U-B | 70–71 | 4 | 1 | M | Olive/black organic mud (TOC) | 7.0 | −20.7 | 39.74 ± 0.22 | 39.48 ± 0.22 | 7413 ± 44 | 7970–7495 | 7740 ± 120 | 7730 | E |
| SUERC-5061 | PQP-30L-B | 81–82 | 3 | 1 | M | Olive grey fine silty mud (TOC) | 0.8 | −19.7 | 38.30 ± 0.22 | 38.05 ± 0.22 | 7709 ± 46 | 8310–7740 | 8020 ± 140 | 8010 | E |
| SUERC-5063 | PQP-41L-B | 92–93 | 2 | 1 | M | Olive/black organic mud (TOC) | 0.9 | −19.6 | 36.31 ± 0.25 | 36.07 ± 0.25 | 8138 ± 56 | 8890–8070 | 8450 ± 180 | 8440 | E |
| SUERC-5064 | PQP-51L-B | 102–103 | 1 | 1 | M | Olive grey fine silty mud (TOC) | 1.3 | −20.7 | 36.50 ± 0.22 | 36.26 ± 0.22 | 8097 ± 48 | 8700–8050 | 8390 ± 160 | 8390 | E |
| SUERC-5067 | PQP-78L-B | 129–130 | 1 | 1 | M | Olive grey fine silty mud (TOC) | 1.4 | −19.7 | 34.76 ± 0.22 | 34.53 ± 0.22 | 8489 ± 51 | 9260–8480 | 8860 ± 190 | 8850 | E |

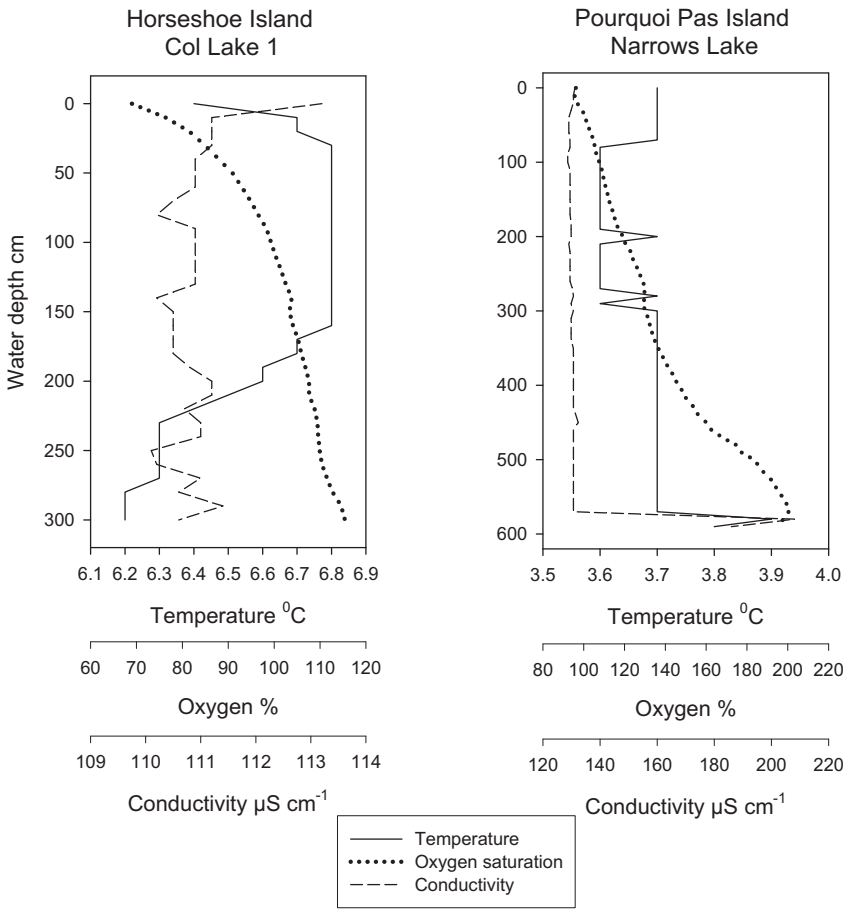


**Fig. 3.** Water column profiles of temperature, oxygen saturation and conductivity in the study lakes. Measurements collected with a SOLOMAT water quality meter using the methods described in Smith et al. (2006). The oxygen measurements should be interpreted with caution due to freezing of the probe membrane during the field campaign.

transition zone (Lithology Unit 2, 72–64 cm) and laminated microbial mats (Lithological Unit 3, 64–0 cm). Zone 3 was divided into 3 sub-zones based on changes in the colour and texture of the microbial mats from dark-olive grey (Lithological Unit 3.1, 64–30 cm) to black (Lithological Unit 3.2, 30–2.5 cm) to grey–brown mats with small 'flake-mats' (Lithological Unit 3.3, 2.5–0 cm).

Radiocarbon dating of the core shows that, with one exception at 94–95 cm, the ages were in stratigraphic order (Table 2, Fig. 5). The living surface of the benthic microbial mat had a measured radiocarbon age of 693 ± 26 $^{14}$C yr BP. This was interpreted as a local carbon reservoir effect and was subtracted (prior to calibration) from the radiocarbon ages obtained from the top 61 cm (Lithological Unit 3) of the core; above the transition from glaciolacustrine sediments to laminated microbial mats. In preliminary age–depth modelling experiments undertaken in Oxcal and CLAM, retention of the reservoir correction into glaciolacustrine sediments below 61 cm resulted in an age reversal. A simple interpolated age–depth model undertaken in CLAM was chosen as best representing the most probable sequence of calibrated ages, with the fewest age–depth reversals, and the lowest log fit values (indicating a better fit to data). More complex models produced similar age–depth profiles.

Paired dates on microbial mats and the >125 µm microbial mat fraction at 2–3 cm yielded calibrated ages within error (Table 2). Triplicate dates on moss macrofossils, *B. gaini* and bulk sediments in the 65–66 cm sample also yielded calibrated ages within error. The oldest date from the bulk glaciolacustrine material at 94–95 cm in Lithology Unit 1 was 30,964 ± 1115 $^{14}$C yr BP; 35,780 (38,650–33,380) cal yr BP. The age range of 34,630–31,370 cal yr BP at 110–111 cm is overlapping, suggesting an elevated sedimentation rate and/or reworking of sediments near the base on the core (Fig. 5).

The oldest macrofossil dated was a moss fragment at 73–74 cm deposited at 10,610 (11,000–10,300) cal yr BP. The Lithological Unit 1 to 2 transition was complete just after 10,490 (10,660–10,270) cal yr BP, and the Lithological Unit 2 to Unit 3 transition after 9090 (9270–8990) cal yr BP. Sediment accumulation rates were relatively rapid between 111 and 86 cm (mean 0.06 mm yr$^{-1}$), low between 86 and 73 cm (mean 0.013 mm yr$^{-1}$) and then increased from 73 to 46 cm (mean 0.057 mm yr$^{-1}$) reaching maximum levels between 46 and 8.5 cm (mean 0.186 mm yr$^{-1}$) then declining between 8.5 and 2 cm (mean 0.063 mm yr$^{-1}$), with a further decline between 2 and 1 cm (0.006 mm yr$^{-1}$) before increasing again in the top 1 cm (0.025 mm yr$^{-1}$) (Fig. 5).

In Lithological Unit 1, the sediment dry mass was between 88 and 48%, and the organic content, measured as TC and $LOI_{550}$, was below 0.4% and 1.7% respectively (Fig. 4). At c. 85 cm, 28,830 (29,370–28,320) cal yr BP there is a small increase in carbonate content, and the first appearance of aquatic mosses which peak at 73 cm. At 81 cm, 21,110 (21,500–20,730 interpolated) cal yr BP *Branchinecta gaini* eggs were present for the first time. In Lithological Unit 2 a lithological transition from glaciolacustrine to lacustrine sediments occurred and was marked, in particular, by increased relative abundances of aquatic mosses, and *Branchinecta gaini* eggs, reaching their peak abundances at 73 cm, 10,550 (10,690–10,400) cal yr BP and 65 cm, 9100 (9200–9000 interpolated) cal yr BP respectively.

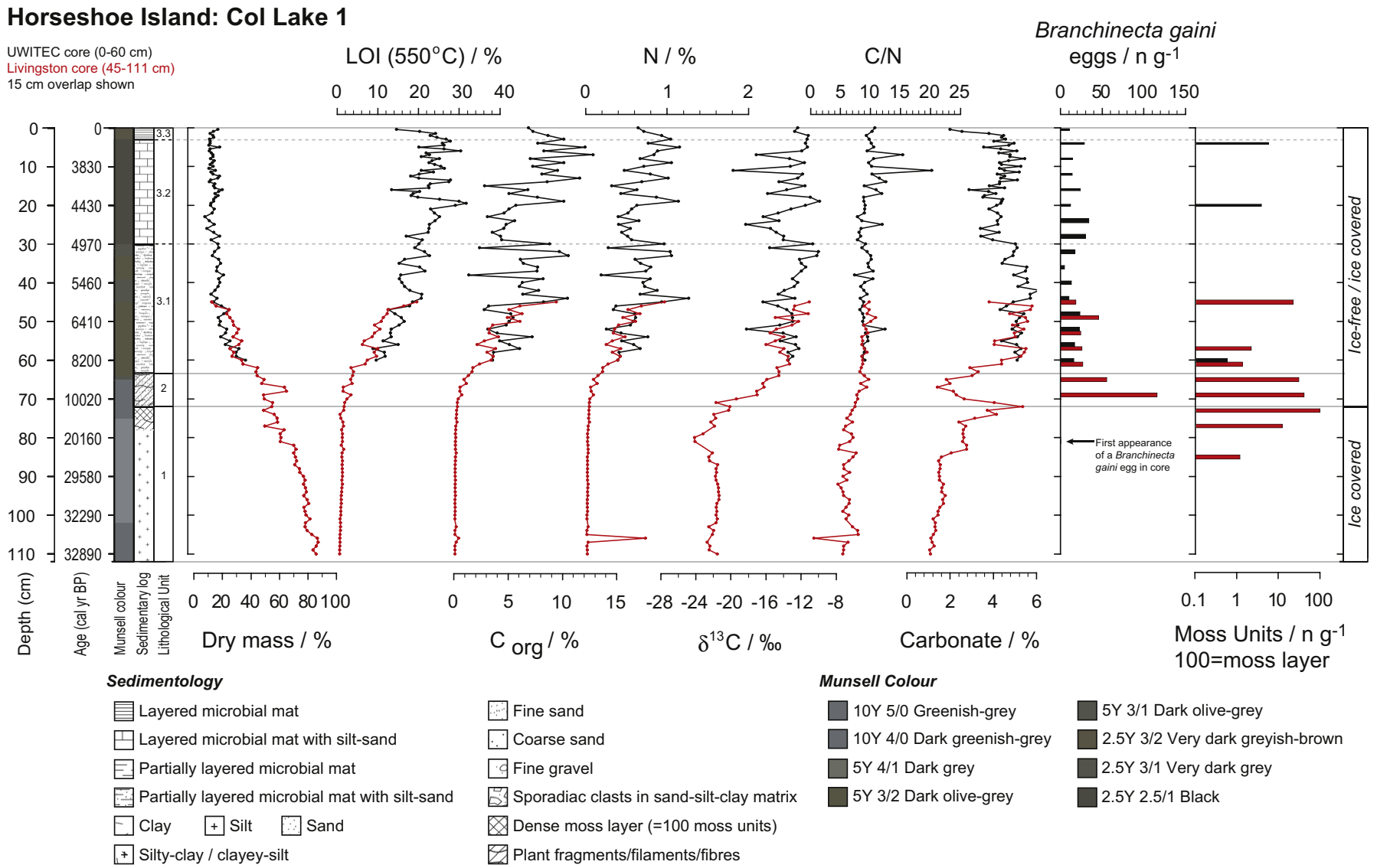


**Fig. 4.** Stratigraphic analyses of the 1.11 m lake sediment core from Col Lake 1, Horseshoe Island including sedimentary logs, physical properties and the presence of moss macrofossils and eggs of the fairy shrimp *Branchinecta gaini*.

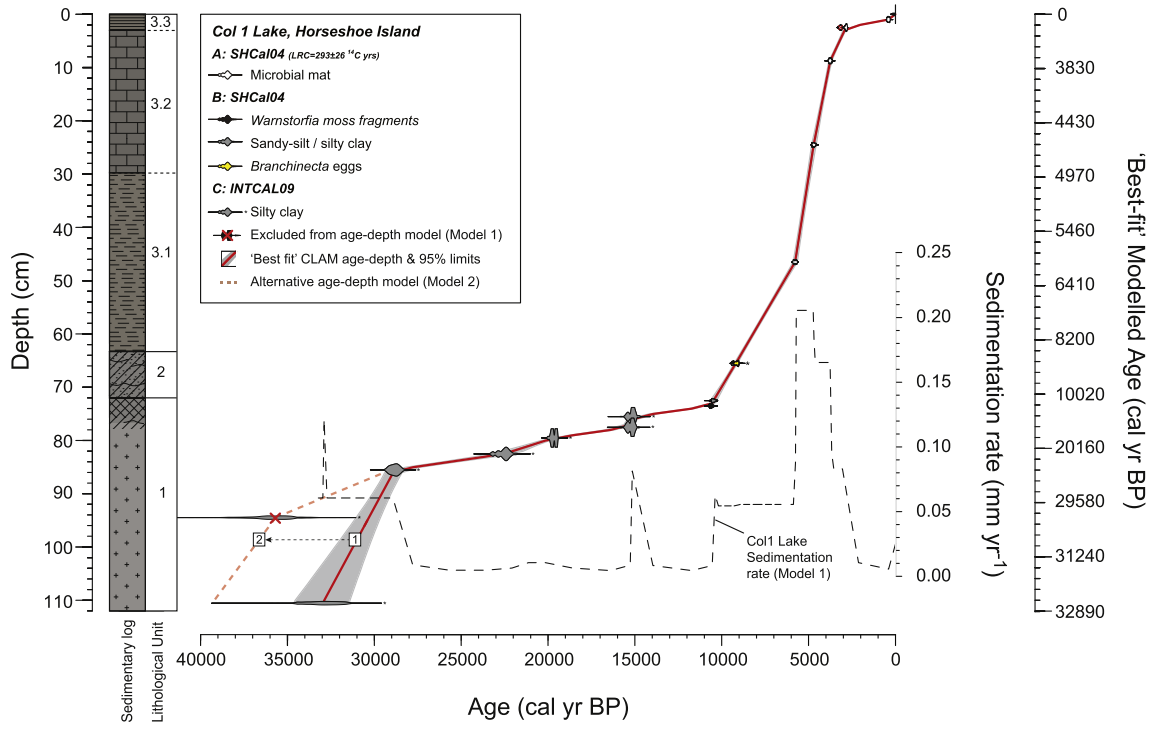


**Fig. 5.** Radiocarbon age depth models and sediment accumulation rates for the Col Lake 1 sediment core from Horseshoe Island. One outlier is excluded from age–depth Model 1. The radiocarbon dates at 94–95 cm and 110–111 cm are both in a poorly defined area of the radiocarbon calibration curve and their two age ranges overlap – this means that although their mean ages create an age reversal, they could still be in sequence. Model 2 shows this alternative scenario, which we consider to be less likely.

The transition could be seen in most parameters including decreases in dry mass, increases in organic content, and continuing positive shifts in $\delta^{13}C$ and C/N. Through Lithological Unit 3.1 there were continued decreases in dry mass, increases in TC, $LOI_{550}$, carbonate, $\delta^{13}C$ and C/N. Organic carbon generally exceeded 7.5% between 45 and 30 cm (5700–4970 interpolated best fit ages), 19–18 cm (4310, 4400–4220 interpolated) and 14–2 cm (4070–2030 interpolated best fit ages). Most of these proxies were relatively stable in Lithological Unit 3.2 although there were 2 samples at 7 and 11 cm which had lower $\delta^{13}C$ and higher C/N. The uppermost samples (Zone 3.3) showed a decline in organic content.

Through the core the trajectory of $\delta^{13}C$ and C/N (Fig. 6) shows a shift from values of around −20 to −25‰; associated elsewhere on the Antarctic Peninsula with glaciolacustrine material including gravels and fine grained sediments (Hodgson et al., 2009b, Fig. 6) to values more typical of a cyanobacteria-dominated environment (−10 to −17‰ $\delta^{13}C$; 7–12 C/N) (e.g. Smith et al., 2006).

### 4.2. Pourquoi-Pas Island, Narrows Lake

The Narrows Lake occupies a classic isolation basin setting below the Holocene marine limit at 40.79 m above the present high water mark in The Narrows. The altitude of the sill is 19.41 m above the present high water mark (BAS survey point 31, Hodgson et al., 2003). The lake is seasonally ice free, 125 m long, and 6.2 m deep with benthic and epilithic mats of cyanobacteria and zooplankton including *B. gaini* and *Daphniopsis/Daphnia* sp. Small moss beds are present in the littoral zone. The water chemistry is typical of a polar freshwater oligotrophic lake with little chemical influence from the nearby marine water (Table 1). Profiles of the water column (measured on 21 Jan 2003) showed near stable temperature and conductivity profiles, and increasing oxygen saturation with depth (Fig. 3). At the time of sampling inflow streams were supplying the lake with fresh snow-melt and the lake was discharging over the sill into The Narrows.

The 1.3 m sediment core from the Narrows Lake was divided into five lithological units (Fig. 7), and four significant diatom zones based on a stratigraphically constrained clustering and broken stick analysis (Fig. 8). Lithological Unit 1 (130–98 cm) consisted of dark olive grey fine marine mud coarse sands and fine gravel phasing upwards into black sediments with a coarse sands-silt-clay matrix and sporadic clasts in Lithological Unit 2 (98–91 cm), and olive grey fine marine muds and coarse sand in Zone 3 (91–81 cm). This was overlain by a marked transition to olive grey mud, fine sands and the decayed remains of microbial mats (Lithological Unit 4, 81–61 cm). Above the transition, the core consisted of partially layered microbial mats (Lithological Unit 5, 61–0 cm) with a number of sub-zones based on minor changes in lithology.

Radiocarbon dates were in stratigraphic order with the exception of minor reversals at 20–21 cm and 102–103 cm, the latter of which is within calibrated error (Fig. 9, Table 3). As with Col Lake 1, due to a general lack of age-reversals, a simple interpolated age–depth model was chosen as best representing the most probable sequence of calibrated ages.

The living surface of the benthic microbial mat had a radiocarbon age of 270 ± 40 $^{14}C$ yr BP. This was interpreted as a small local carbon reservoir effect and was subtracted, prior to calibration, from the radiocarbon ages in the top 65 cm of the core, which consisted of similarly laminated freshwater sediments. Paired moss macrofossils and *B. gaini* eggs at 56–57 cm yielded calibrated ages within error. Paired microbial mat and *B. gaini* eggs at 64–65 cm also yielded calibrated ages within error. The oldest dated material in Lithological Unit 1 was 8489 ± 51 $^{14}C$ yr BP or 8850 (9260–8480) cal yr BP. The transition to microbial mats (Lithology Units 4–5) was complete by 64 cm or 7165 (7280–7030) cal yr BP.

Sediment accumulation rates in the Narrows Lake record were relatively high for most of Lithological Units 1–4, with stepped

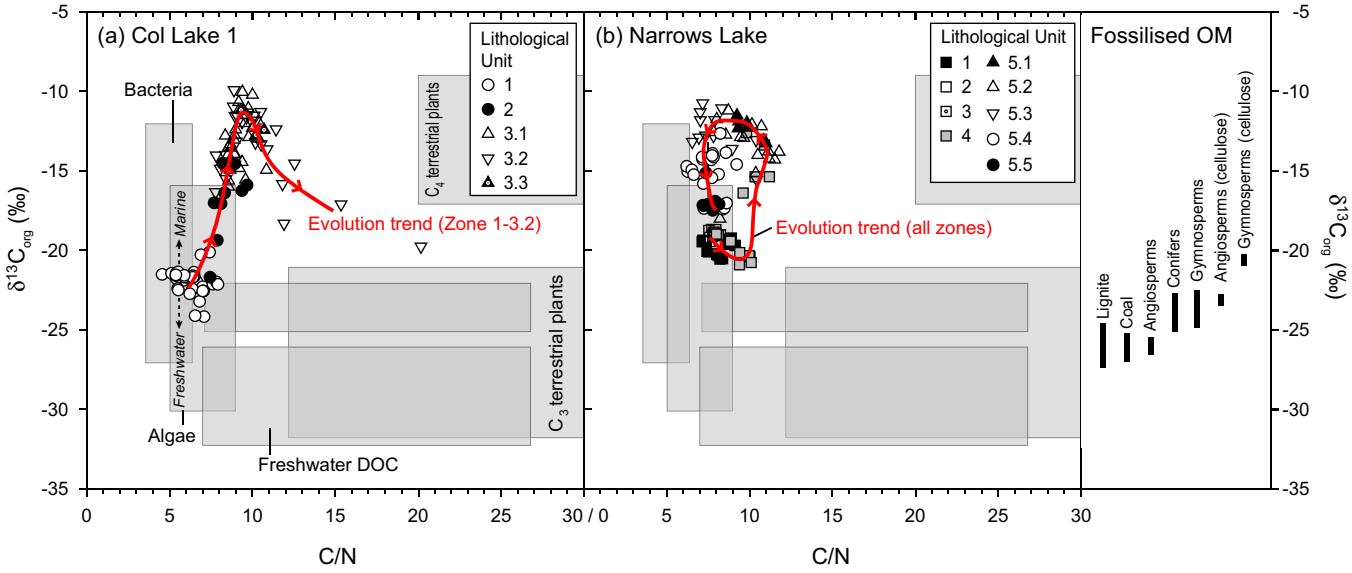


**Fig. 6.** $\delta^{13}C$, C/N biplot, Col Lake 1, Horseshoe Island and the Narrows Lake, Pourquoi-Pas Island (reference data fields from Hodgson et al., 2009a, and references therein).

decreases from a mean of 0.67 mm $yr^{-1}$ in Units 1 and 2 (130–91 cm), to 0.37 mm $yr^{-1}$ in Unit 3 (91–81 cm), to 0.12 mm $yr^{-1}$ in the top half (70–65 cm) of Unit 4. Values decline slightly further in between 65 and 38 cm (mean 0.07 mm $yr^{-1}$), before increasing between 38 and 21 cm (mean 0.16 mm $yr^{-1}$), decreasing between 20 and 10 cm (0.08 mm $yr^{-1}$) then increasing again in the top 10 cm (0.17 mm $yr^{-1}$) (Fig. 9).

In Lithological Units 1–3 (130–81 cm) the mean dry mass was 41%, organic content, measured as TC and $LOI_{550}$ remained below 3% and 5% respectively and carbonate ($LOI_{950}$) was relatively stable around 2.5% (Fig. 7). $\delta^{13}C$ values were generally below −18‰ and C/N ratios remained between 6 and 10 (Fig. 6). In the early phases of the transition to microbial mats in Lithological Unit 4 (81–61 cm) most parameters showed marked shifts including peaks in organic carbon (17%), carbonate content (4%), positive shifts in C/N, and the first appearance of aquatic mosses and *Branchinecta gaini* eggs. During the transition, there was a brief decline in organic carbon, carbonate and nitrogen. Above the transition, in Lithological Unit 5.1 (60–57 cm; 6450–6100 cal yr BP interpolated best fit age), organic content again increased to above 10%. In Lithological Units 5.2–5.3, and part of Lithological Unit 5.4 (57–27 cm; 6200–2630 interpolated best-fit age) organic content continued to exceed 5%. Lithological Unit 5.2 also had a number of thick moss layers, and related high C/N ratios, a peak in the concentration of *B. gaini* eggs, and a positive shift in $\delta^{13}C$. Through Lithological Units 5.4–5.5 (33–0 cm; 3010–14 cal yr BP interpolated best fit age) TOC values declined to a mean of 3.5%, there was a steady decrease in the concentration of *Branchinecta gaini* eggs, a near absence of mosses above 20 cm (2100, 2250–2000 cal yr BP interpolated) and a slight negative shift in $\delta^{13}C$. The trajectory of $\delta^{13}C$ and C/N (Fig. 6) showed a separation of the carbon sources in Lithology Units 1–3 from those in Lithological Unit 4 and in Lithological Unit 5.

Diatoms recorded a transition from marine to brackish, then lacustrine taxa (Fig. 8). Diatom Zone 1 (127–68 cm) was dominated by *Chaetoceros* resting spores, *Nanofrustulum shiloi*, and a *Pseudostaurosira* species. Within Diatom Zone 2 (68–54 cm) the transition from marine sea ice sub-surface communities to freshwater taxa was complete by 65–64 cm, 7165 (7280–7030) cal yr BP. *Navicula phyllepta* was relatively abundant in this transition zone and has been recorded in similar isolation basin transitions in east Antarctica (Verleyen et al., 2004, 2005). The freshwater diatom community was highly variable between 65 and 54 cm with a succession from communities dominated by *Pinnularia microstauron*, to assemblages dominated by *Navicula veneta* and *Planothidium quadripunctatum*, culminating in a flora in which *Gomphonema* spp. and *P. microstauron* were abundant. Diatom Zone 3 (54–22 cm) was dominated by an unknown Naviculoid species, as yet not reported from other Antarctic lakes (Van de Vijver et al., 2002; Verleyen et al., 2003). From 42 cm upwards (3890, 4000–3790 interpolated) the relative abundance of *Psammothidium subatomoides* gradually increased. *Gomphonema* spp. slightly decreased in Diatom Zone 4 (22–0 cm). Stomatocysts reached a maximum relative abundance at 18 cm and *Naviculadicta elorantana* appeared for the first time in the core. *Diadesmis langebertalotii*, which was also present in the transition zone, became subdominant in the most recent sediments. *Gomphonema* spp. increased in the top 1 cm of the core.

### 4.3. Raised beaches

Raised beach surveys at Horseshoe Island, Pourquoi-Pas Island and Calmette Bay (Fig. 10) showed remarkably similar profiles (Fig. 10), but with an offset at Pourquoi-Pas Island where the survey incorporated the Narrows Lake isolation basin. The surveys identified the highest marine limits at Pourquoi-Pas Island (40.79 m above the present high water mark) and Calmette Bay (40.55 m). The beach surveyed at Gaul Cove on Horseshoe Island was present up to a height of 22.11 m, above which there was an indistinct rock shoreline which was not surveyed.

At Pourquoi-Pas Island, the raised shoreline included a number of steps or terraces, presumably built up by wave action, and outcrops of local bedrock which have undergone significant coastal erosion. The first prominent step occurs between 32.68 m and 39.28 m, and is present in some areas as a smoothed rock platform at 32.68 m and in others as the vertical limit of large (c. 150 mm) rounded boulders. The second is a platform at 21.49 m, which extends around the immediate lake catchment, at ca 2.69 m above the maximum lake water level. Both can be traced as continuous features around the immediate coastline. In contrast, the raised beaches at Calmette Bay consisted of a vertical sequence of beaches with much larger (45–65 cm diameter) and more rounded large beach clasts. Although survey time was limited, the largest clasts

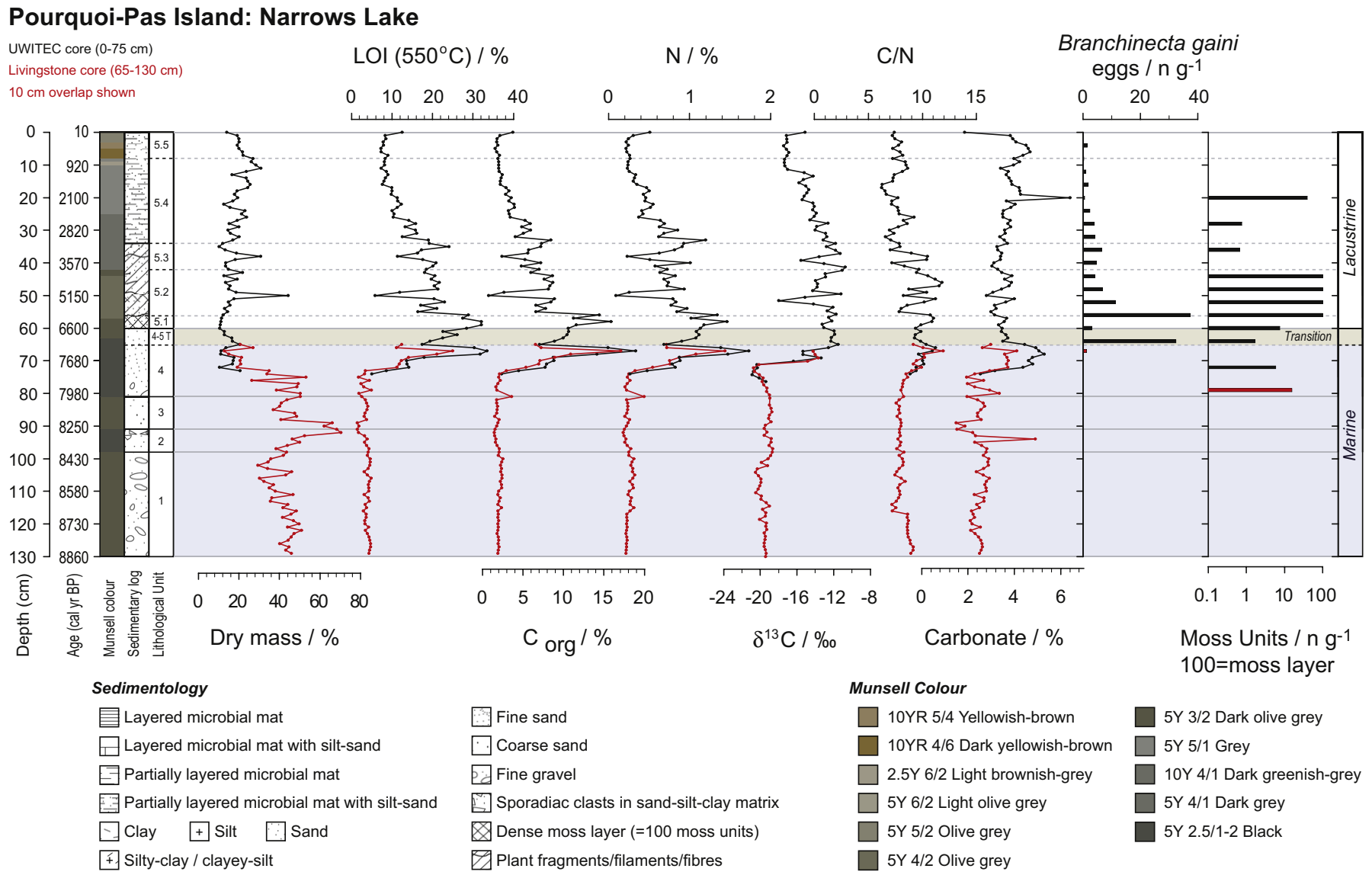


**Fig. 7.** Stratigraphic analyses of the 1.3 m lake sediment core from the Narrows Lake, Pourquoi-Pas Island including sedimentary logs, physical properties and the presence of moss macrofossils and eggs of the fairy shrimp *Branchinecta gaini*.

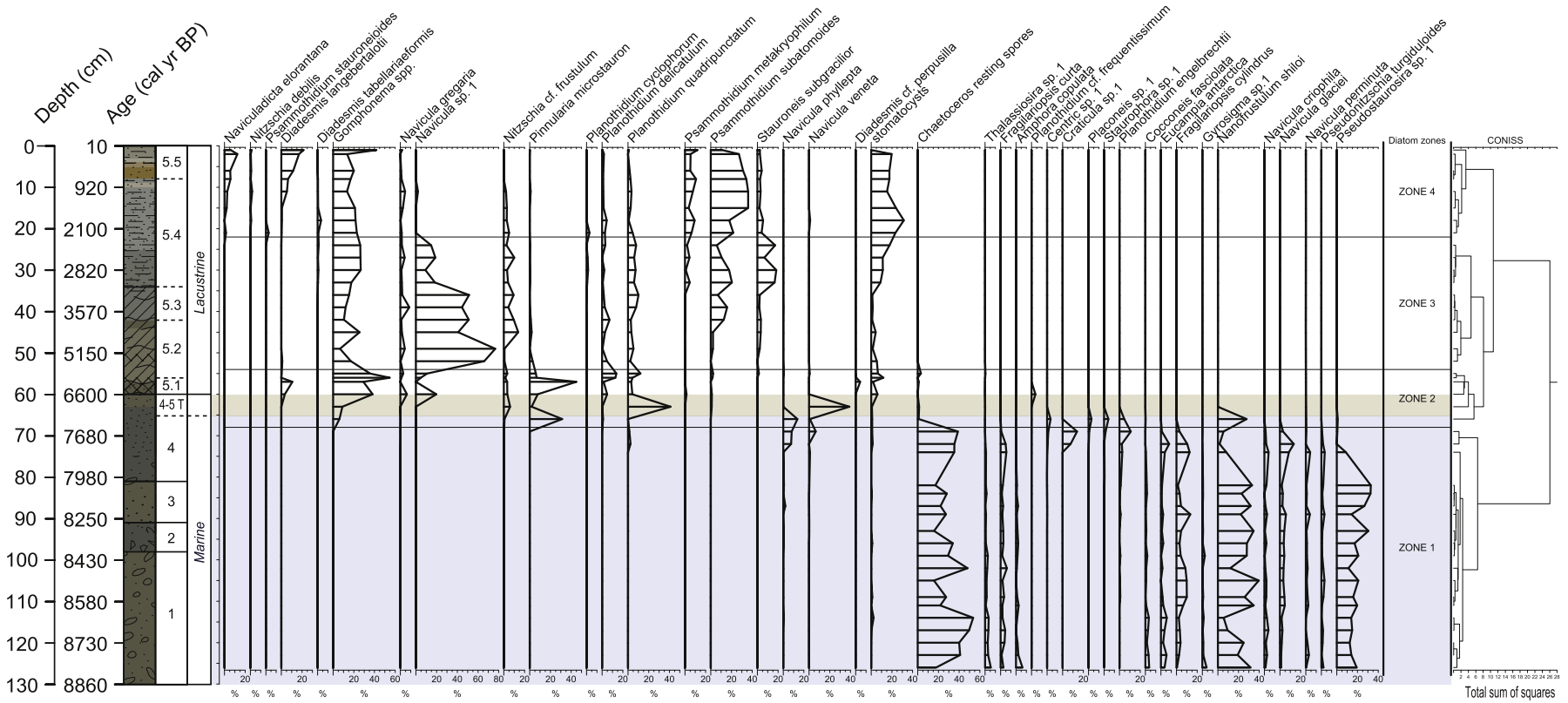


**Fig. 8.** Diatom stratigraphy of the Narrows Lake sediment core including statistically significant diatom zones. Marine diatom taxa are grouped to the right of the diagram, and freshwater to the left. Only species with a relative abundance exceeding 2% are shown.

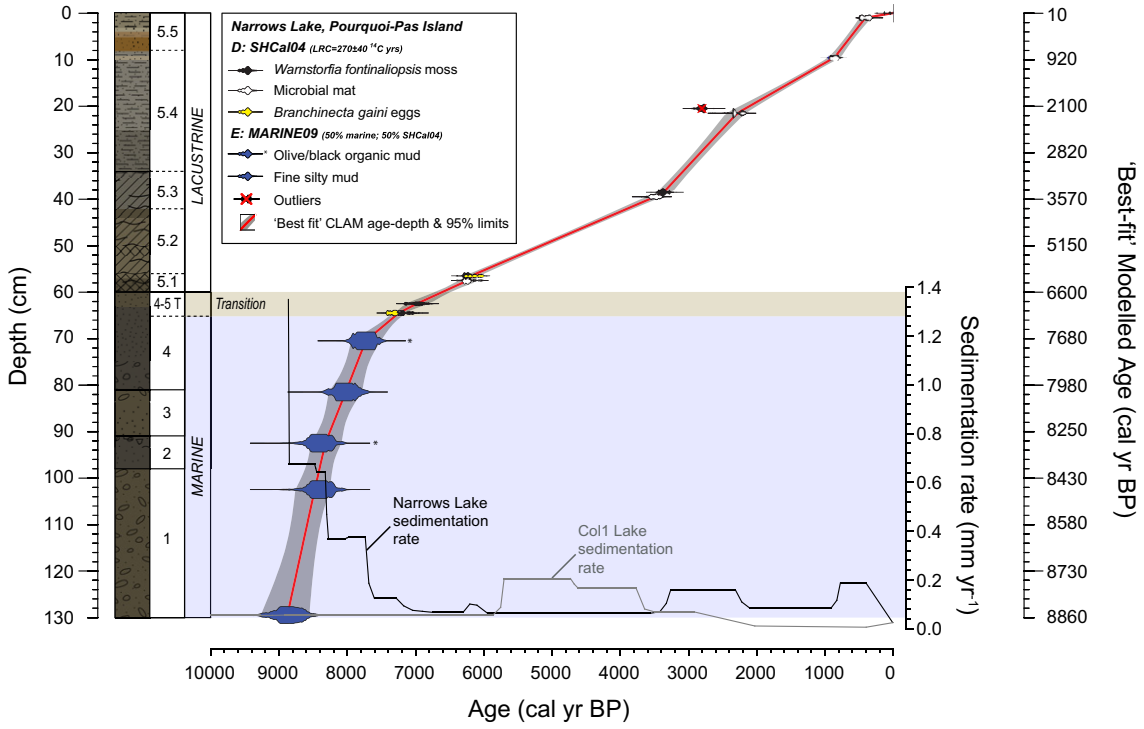


**Fig. 9.** Radiocarbon age–depth model for the Narrows Lake sediment core from Pourquoi-Pas Island, with sediment accumulation rates for Narrows Lake and Col 1 Lake.

were observed between 30.6 and 32.6 m above the high water mark. At Horseshoe Island beach clast composition and roundness were measured up to 22.11 m above the high water mark. Both clast size and roundness were at maxima between c. 4 and 10 m above the present high water mark (Fig. 11).

## 5. Discussion

The data presented provide a number of new constraints on the glacial and environmental history of the Marguerite Bay region.

First, the radiocarbon ages suggest that glacial sediments in the Col Lake 1 sediment core from Horseshoe Island were mostly deposited in stratigraphic order through the Last Glacial Maximum (with one exception). If no natural 'contamination' by an old carbon reservoir, such as glacial meltwater or geological sources (e.g., Roberts et al., 2008), was present at this site when the glacial sediments were deposited, this would suggest that the Col area was subject to a non-erosive glacial regime from 35,780 (38,650–33,380) or 32,910 (34,630–31,370) cal yr BP onwards. Analysis of aerial photographs shows that in its current configuration local glaciers are diverted away from the Col 1 site via the deep glacial trough occupied by the Shoesmith Glacier (Fig. 1d and 2a), and the archipelago is positioned between major ice stream outlets in northern Marguerite Bay (Fig. 1c); so this conclusion is not unreasonable from a glaciological perspective.

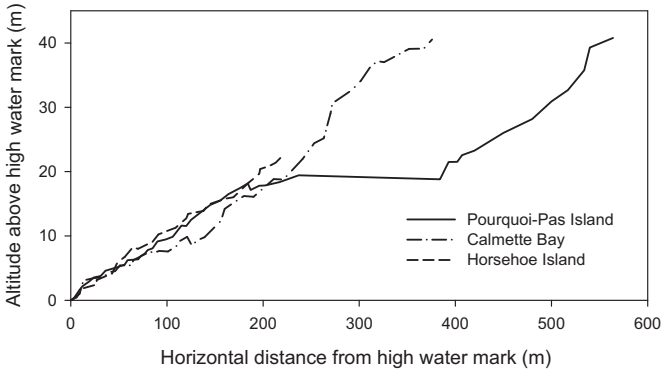


**Fig. 10.** Raised beach profiles from (a) Horseshoe Island, showing raised beaches in Gaul Cove which were surveyed form 67° 49.563′ S, 67° 12.869′ W to 67° 49.613′ S, 67° 13.166′ W (b) Pourquoi-Pas Island, where raised beaches and terraces were surveyed from c. 67° 35.52′ S, 67° 11.51′ W to c. 67° 36.02′ S, 67° 12.36′ W at a bearing of 194°, from the coast to the Holocene marine limit across the long axis of the Narrows Lake and (c) Calmette Bay, which was surveyed from 68° 03.848′ S, 67° 10.419 W to 68° 04.040′ S, 067° 10.532′ W. For photographs of the locations of the profiles see Fig. 2d–f.

Second, the earliest onset of deglaciation, or a deglaciation event, on the raised central area on Horseshoe Island is suggested by the presence of moss fragments embedded within the sediment matrix at 28,830 (29,370–28,320) cal yr BP. These radiocarbon dates are amongst the earliest reported for the region; hence, we cannot completely rule out that the bulk sediment dates in this zone are influenced by a carbon reservoir from glacial meltwater or geological sources (e.g., Roberts et al., 2008). However, the consistent stratigraphic order of the ages, at least after 28,830 (29,370–28,320) cal yr BP (Table 2) and the lack of old carbon in the predominately volcanic bedrock possibly argues against this. The dates are also of terrestrial origin and, therefore, presumably not influenced by marine radiocarbon reservoir effects. Because a cluster of similar bulk glacial sediment radiocarbon ages have been reported elsewhere in the region the spatial and temporal pattern of their occurrence requires further examination. For example, in the Bellingshausen Sea (Fig. 1) there are a series of radiocarbon dates that suggest that initial ice retreat from the shelf edge may have started as early as c. 30,000 cal yr BP (Hillenbrand et al., 2010), which is in broad agreement with cosmogenic isotope evidence from Moutonnée Valley (340 km to the south), that suggests ice thinning commenced there after c. 30,000 years BP (Bentley et al., 2006). These events immediately post-date Antarctic Isotopic Maximum 4 seen in the EPICA Dronning Maud Land and EPICA Dome C and other Antarctic ice cores at c. 35,000–30,000 yr BP (EPICA, 2006).

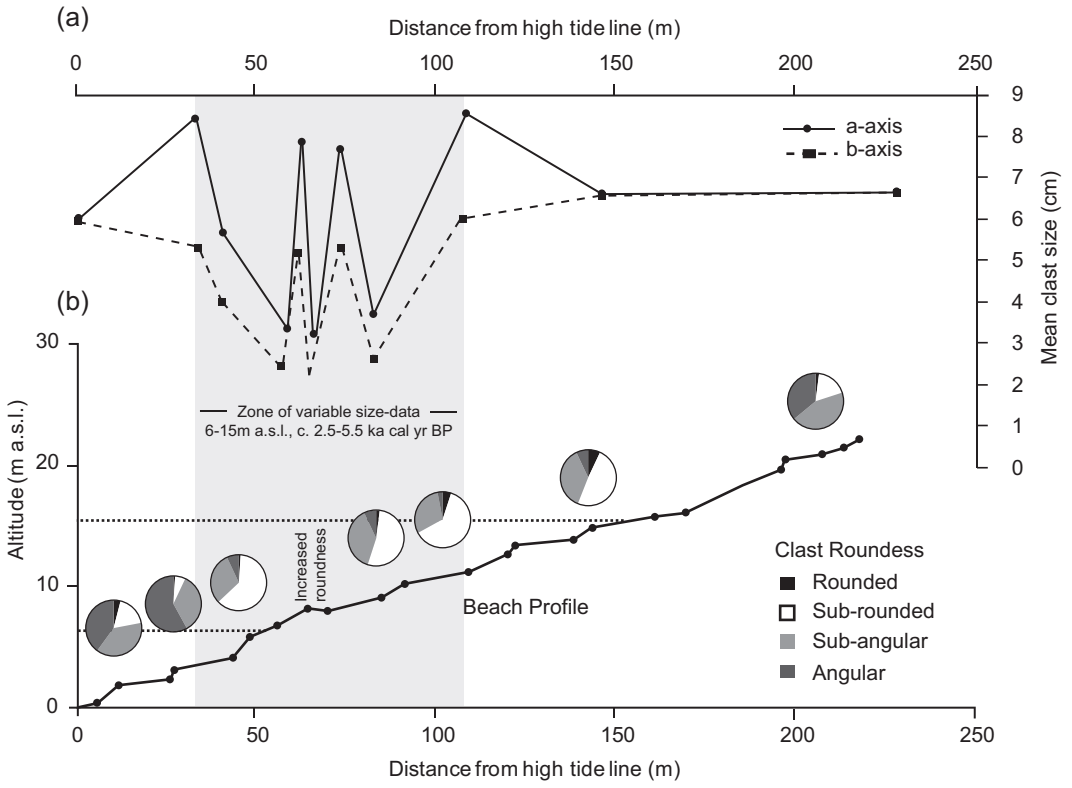


**Fig. 11.** (a) Clast size and (b) clast roundness data from the surveyed raised beaches in Gaul Cove, Horseshoe Island.

The next potential evidence of onset of deglaciation, or a deglaciation event, is the colonisation of the Col 1 site by *B. gaini*, which is present (as eggs) in the sediment matrix from 81 cm, 21,110 (21,510–20,730 interpolated) cal yr BP. The latter indicates the existence of a perennial water body. If correct, this would require at least one part of the ice sheet in inner Marguerite Bay to be less than 140 m thick (relative to present sea level) at this time. This event coincides with continued ice thinning at Moutonnée Valley (Bentley et al., 2006), and occurs shortly after the retreat of ice in the Bellingshausen Sea, which reached the mid shelf by 23,600 cal yr BP (Hillenbrand et al., 2010). On land, cosmogenic isotope exposure ages from NW Alexander Island and Rothschild Island show progressive ice thinning since at least 22,000 yr BP, reaching an elevation of c. 440 m by 10,200–11,700 yr BP (Johnson et al., 2012).

Further evidence of warming and deglaciation at this time comes from further north in the Scotia Sea (Collins et al., 2012) where both the winter sea ice and summer sea ice edges experienced a rapid melt back event between 23,500 and 22,900 cal yr BP. South, in the western Amundsen Sea Embayment, deglaciation was probably underway as early as 22,351 cal yr BP (Smith et al., 2011). These events coincide with, or immediately post-date Antarctic Isotopic Maximum 2 (~23,500 cal yr BP) seen in Antarctic ice cores (EPICA, 2006) and Southern Ocean SST records (Kaiser et al., 2005).

All of these radiocarbon ages pre-date ice core evidence, which show the onset of post-Last Glacial Maximum deglaciation from c. 18,000 yr BP (Masson-Delmotte et al., 2011) and marine geological evidence, which show the onset of ice retreat in the northern Antarctic Peninsula ~18,000 cal yr BP (e.g. 17,340 cal yr BP in Bransfield Basin (Heroy and Anderson, 2005). Further south in outer Marguerite Bay the earliest deglaciation of Rothschild Trough (site GC514) was at 14,430 cal yr BP (16,537 $^{14}$C yr BP) and Charcot Trough (site GC471) occurred at 13,490 cal yr BP (15,564 $^{14}$C yr BP) (Graham and Smith, 2012). In the Bellingshausen Sea, the ice had reached the inner shelf by 14,300 cal yr BP (Hillenbrand et al., 2010). Studies of marine sediment cores within Marguerite Trough document a two-stage retreat of the Last Glacial Maximum Ice Stream across the continental shelf (Ó Cofaigh et al., 2005; Kilfeather et al., 2011). The first stage of retreat began shortly before 14,210 cal yr BP and 13,090 cal yr BP (Heroy and Anderson, 2007; Bentley et al., 2011) at the outer shelf with the ice retreating approximately 200 km before stabilising. This retreat event has been linked to the rapidly rising sea levels of Meltwater Pulse 1A destabilising the grounding line.

Unequivocal evidence of the onset of Holocene deglaciation on land is provided by the presence of an aquatic moss fragment with sufficient carbon for AMS radiocarbon dating at 73–74 cm which grew in the Col Lake 1 at 10,610 (11,000–10,300) cal yr BP. The establishment of moss is followed by a peak abundance of *Branchinecta gaini* eggs from 69 cm, 9830 (9940–9720 cal yr BP interpolated). This is accompanied by an increase in sediment water content (i.e. decrease in dry mass) and a positive shift in $\delta^{13}$C suggesting a freshwater biota was well established at this time. These latter deglaciation ages are reasonably consistent with the Narrows Lake core, situated at a lower altitude and closer to the Antarctic Peninsula Ice Sheet, where the onset of marine sedimentation was at or before 8850 (9260–8480) cal yr BP (Table 2).

The onset of marine sedimentation at the Narrows Lake site provides a lower ice thickness constraint at 19.41 m a.s.l. for the rapid deglaciation of the nearby ridge at Parvenu Point, which, based on cosmogenic isotope dating (Bentley et al., 2011), had been exposed down to 75 m above present sea level at 9600 yr BP. Collectively, these data support the inference of a rapid thinning of the Marguerite Trough Ice Stream within the Marguerite Bay archipelago (Bentley et al., 2011) at this time. Furthermore, the transition from glaciolacustrine to full lacustrine conditions at Col

Lake 1 on Horseshoe Island between 10,490 (10,660–10,270) and 9090 (9270–8990) cal yr BP provides further evidence that the same rapid ice thinning and deglaciation occurred throughout the northern Marguerite Bay archipelago, supporting the interpretation that this ice thinning at the margins of Marguerite Bay records the regional thinning and retreat of the Marguerite Trough Ice Stream (Bentley et al., 2011). This interpretation is also consistent with marine geological evidence for the deglaciation of Neny Fjord in inner Marguerite Bay at, or prior to, 9040 cal yr BP (Allen et al., 2010). These events have been collectively linked to the influx of warm circumpolar deep water onto the continental shelf (Allen et al., 2010; Kilfeather et al., 2011) and possibly the end of the early Holocene temperature maximum in ice cores triggering the second stage of deglaciation (Bentley et al., 2011) and the early Holocene retreat of the George VI Ice Shelf southwards past Ablation Point after c. 9600 cal yr BP (Bentley et al., 2005b; Smith et al., 2007b; Roberts et al., 2008).

Third, because deglaciation was accompanied by relative sea level change, we can indirectly infer the relative thickness of the Antarctic Peninsula Ice Sheet from the altitude of the early Holocene relative sea level maximum. In the northern Antarctic Peninsula at Beak Island, the relative sea level maximum was 14.91 m above present at c. 8000 cal yr BP (Roberts et al., 2011), in the South Shetland Islands (adjacent to the Antarctic Peninsula Ice Sheet) the relative sea level was c. 20 m above present at 7360–7000 cal yr BP (Fretwell et al., 2010; Watcham et al., 2011), whilst in Marguerite Bay it was between 40.79 m (Pourquoi-Pas Island) and 40.55 m (Calmette Bay) sometime after 9000 cal yr BP. This is significant for two reasons: first, it implies that the Lateglacial ice mass was thicker along the margins of Marguerite Bay compared with the more northerly sites (above); second, that the rapid thinning of this ice mass resulted in a relatively fast isostatic recovery, outpacing eustatic sea level rise sometime after 9000 cal yr BP. Recent optically stimulated luminescence data on beach cobbles in Calmette Bay (Simkins pers. comm.) suggest that the upper terraces may pre-date the Last Glacial Maximum which would be consistent with the pre-Last Glacial Maximum thinning events that our data suggest during Antarctic Isotopic Maxima 1 and 2.

The transition from marine sediments to freshwater lake sediments, identified by diatom analysis was complete by 65–64 cm, in the Narrows Lake provides a relative sea level constraint of 19.41 m at 7270 (7385–7155) cal yr BP (based on 6705 ± 42 $^{14}$C yr BP with Local Reservoir Correction (LRC) of 270 ± 40 $^{14}$C yr BP included, Table 3). This is a minor revision to the provisional radiocarbon age (Beta-180801; Table 3) of the most prominent moss layer at a stratigraphic depth of 59–60 cm in the Livingston core, first published in Bentley et al. (2005a), which produced minimum isolation age of 7000 (7150–6840) cal yr BP (6420 ± 50 $^{14}$C yr BP calibrated using calibration model 'D', Table 3, with a LRC of 270 ± 40 $^{14}$C yr BP included). We have subsequently revised the stratigraphic depth of this sample to 62–63 cm based on more precise alignment of proxy data, rather than preliminary field depths and identification of the transition, which was based on changes in sediment lithology alone (Bentley et al., 2005a). The revised age results in a slightly faster mean early Holocene/pre-isolation uplift rate of 12.5 mm yr$^{-1}$ (assuming the 9000 cal yr BP extrapolated age of the 41 m relative sea level maximum on Pourquoi-Pas Island in Bentley et al. (2005a) is correct), and a mean post-isolation rate of 2.7 mm yr$^{-1}$. A nearby relative sea level constraint showing an uplift rate of 3.1 mm yr$^{-1}$ (14.4 m fall in RSL in the last c. 4.6 ± 0.4 ka) on Alexander Island (Roberts et al., 2009) is also broadly consistent with these data, as are some glacial isostatic adjustment models (e.g. Peltier, 2004; Bassett et al., 2007; Whitehouse et al., 2012).

Fourth, collectively, the raised beach data and the lake sediment core data give information on Holocene climate change. Observations of increased clast sizes and clast roundness on the surveyed beaches provide evidence of periods of increased wave energy, likely related to reductions in summer sea-ice extent (e.g. Bentley et al., 2005a). At Calmette Bay, the marked occurrence of the largest (c. <130 cm, long axis) and most rounded clasts (between 30.6 and 32.6 m) above the high water mark can be dated (via cross reference to the regional relative sea level curve (Bentley et al., 2005a)) to approximately 8000 corrected $^{14}$C yr BP (c. 8250–8742 cal yr BP). This coincides with early Holocene evidence from Neny Fjord (c. 45 km distant from Col Lake 1), which shows a maximum in the abundance of warm open-ocean and meltwater-related diatoms between c. 9000 and 7000 cal yr BP (Allen et al., 2010).

Because of the widespread ecological changes in the Narrows Lake sediment core following isolation from the sea (Lithological Zones 4–5.1), and the likely utilisation of the marine nutrient pool by the newly established freshwater flora following isolation its sensitivity to Holocene temperature-related changes is only considered in Lithological Zones 5.2–5.5 and Diatom Zones 3–4. It is likely that the increase in organic carbon, which exceeds 5% between 6200 and 2630 cal yr BP, is a response to climate warming. This encompasses three periods in the Col Lake 1 sediment core where organic carbon is generally >7.5% (5700–4970, 4370–4310 and 4070–2030 interpolated best fit ages). These are likely related to periods of reduced summer lake ice cover stimulating production in the lake, and collectively suggest regional warming occurred sometime between 6200 and 2030 cal yr BP (Narrows Lake and Col Lake 1 age constraints respectively). The onset of this warming pre-dates the onset of mid-Holocene warming in some other terrestrial records in the northern Antarctic Peninsula (Hodgson et al., 2004; Bentley et al., 2009; Sterken et al., 2012), but ends at a similar time. In the marine geological record from nearby Neny Fjord less pervasive sea-ice cover and long diatom growing seasons are inferred from c. 7000 to 4000 cal yr BP and increased meltwater discharge from c. 4000 to 2800 cal yr BP; both consistent with climate warming at this time. However, there is a mismatch in Col Lake 1 between the *Branchinecta gaini* concentrations (which elsewhere in the region have matched other production indicators (Jones et al., 2000)) and the TOC content. Instead, in these lakes the presence of *Branchinecta gaini* seems to have been most closely associated with the presence of mosses during the transition from glaciolacustrine to lacustrine conditions.

Further evidence of mid- to late-Holocene warming is provided by a period of increased clast sizes (2.5–8.5 cm) and roundness at Horseshoe Island between c. 4 and 10 m a.s.l., which can be approximately dated via cross reference to the regional relative sea level curve (see Bentley et al., 2005a) to a period between 5500 and 2500 $^{14}$C yr BP (c. 6010–5720 to 2300–2010 cal yr BP). This is likely the same event that is recorded in beaches on Rothera Point and Anchorage Island which show more rounded beach material between c. 4.5 and 8 m a.s.l. (Bentley et al., 2005a), estimated from the RSL curve as between c. 3500 and c. 2400 $^{14}$C yr BP (c. 3530–3250 to 2190–1870 cal yr BP), suggesting that there was a period of greater wave activity in the mid Holocene during the formation of these intermediate beaches. The increased wave activity is likely related to reduced summer sea-ice cover. Evidence from Neny Fjord suggests that between c. 4000 and 2800 cal yr BP there was a period of more intense or more proximal glacier discharge events (Allen et al., 2010). Both events are broadly synchronous with the warm, humid mid to late Holocene conditions inferred from records elsewhere in the Antarctic Peninsula region (Ingólfsson and Hjort, 2002; Hodgson et al., 2004; Bentley et al., 2009), for example at Beak Island between c. 3169 and 2120 cal yr BP (Sterken et al., 2012) and in the maritime Antarctic at Signy Island between c. 3800 and 1400 cal yr BP (Hodgson and Convey, 2005).

The decline in organic carbon from 2630 to 2030 cal yr BP (Narrows Lake and Col Lake 1 age constraints respectively) is interpreted as evidence of the onset of Neoglacial conditions. This corresponds to a return to smaller sub-angular clasts on the Horseshoe Island raised beach after c. 2190–1870 cal yr BP (2400 $^{14}$C yr BP; estimated from the RSL curve (see above)), and is consistent with cooler conditions reported in Neny Fjord after c. 2800 cal yr BP (Allen et al., 2010), based on a shorter growing season indicated by diatoms and reduction in the overall biogenic content of the sediment. In the Col Lake 1 record from Horseshoe Island, there is a marked decline in organic carbon and in sediment accumulation rates, or absence of sedimentation, sometime after 2030 (2110–1970) cal yr BP. This may be a result of the nearby snow bank expanding across the lake during the Neoglacial.

The diatoms in the Narrows Lake core provide further information on palaeoenvironmental conditions, in addition to identifying the marine to freshwater transition. The dominance of *Chaetoceros* resting spores, which are amongst the most abundant siliceous microfossils in coastal Antarctica (Armand et al., 2005), in Diatom Zone 1 is considered an indicator of high productivity and stratified surface waters resulting from sea ice melt (Leventer et al., 1996). The other dominant species in this zone are *N. shiloi*, a cosmopolitan euryhaline taxon and found in coastal and littoral environments (Round et al., 1999), including saline and brackish lakes in the Prydz Bay region of east Antarctica (Sabbe et al., 2003) and a *Pseudostaurosira* species for which there is little autoecological information in Antarctica. Following isolation in Diatom Zone 2, freshwater taxa dominate. However, *D. langebertalotii*, which was also present in Diatom Zone 2, as well as *N. elorantana*, increase from 12 cm, 1150 (1230–1080) interpolated cal yr BP, and become subdominant in the most recent sediments from c. 460 (540–380) interpolated cal yr BP. *D. langebertalotii* is currently found in slightly acidic soils which are often influenced by marine animal input (Van de Vijver et al., 2002), which leads to higher nutrient concentrations. *N. elorantana* appears slightly earlier in the core (from 20 cm onwards, after 2100, 2250–2000 interpolated cal yr BP) and is a dominant diatom in seal wallows in the Prince Edward Islands (Van de Vijver et al., 2008). This might suggest an increase in the number of birds and seals visiting the catchment, which is consistent with a marked deviation back towards marine sediment values in the $\delta^{13}$C C/N biplot (Fig. 6).

This evidence is consistent with the occurrence of a radiocarbon dated seal hair embedded in the beach at the Narrows Lake which has a conventional radiocarbon age of 2970 ± 40 $^{14}$C yrs BP (Beta-178164, Bentley et al., 2005a) (calibrated median age 1640 cal yr BP, 95.4% range 1890–1380 cal yr BP using Oxcal v. 4.1, MARINE09 (100% marine) and a $\Delta R$ value of 900 ± 100, which is equivalent to the 1300 ± 100 yr correction applied in Bentley et al. (2005a). The evidence is also consistent with a radiocarbon dated penguin feather embedded in the raised beach at Horseshoe Island with a conventional radiocarbon age of 2310 ± 40 $^{14}$C yrs BP (Beta-178162, Bentley et al., 2005a) (calibrated median age 1130 cal yr BP, 95.4% range 1400–830 cal yr BP using Oxcal v. 4.1, MARINE09 (100% marine) and a $\Delta R$ value of 730 ± 130, equivalent to the 1130 ± 134 yr correction applied in Bentley et al. (2005a); note: calibrating these two ages using the $\Delta R$ smaller value of 664 ± 10 used in this paper produces a maximum likely calibrated median age and 95.4% age range for the seal hair (Beta-178164) of 1920 and 2040–1810 cal yrs BP, and, for the penguin feather (Beta-178164), 1205 and 1290–1100 cal yr BP), and macrofossil evidence that nearby Ginger Island (60 km distant) and Rothera Point (40 km distant) were colonised by Adélie penguins from 2430 to 3170 cal yr BP respectively; although the earliest colonies had been established in Marguerite Bay (Lagoon Island, 42 km distant) from 5380 cal yr BP (Emslie, 2001).

Another finding of note is that *Gomphonema* species become abundant in the top centimetre of the Narrows Lake sediment core, sometime after 410 (490–320) interpolated cal yr BP. This may be, together with the increase in LOI and TOC, related to a response to the earliest onset of late Holocene warming of the Antarctic Peninsula, documented as starting at c. 500–600 cal yr BP by Sterken et al. (2012) and later confirmed by Mulvaney et al. (2012); superimposed on this is the recent rapid instrumental warming. This is consistent with the renewed onset of sedimentation in the Col Lake 1 sediment core at or after c. 400 (490–310) interpolated cal yr BP, and evidence of an increase in sea-ice, open ocean and autumn bloom diatom species (similar to that experienced during the early-Holocene climate optimum) in the Neny Fjord marine sediment record sometime after 200 cal yr BP (Allen et al., 2010).

## 6. Conclusions

This paper provides a new terrestrial perspective on the glacial, sea level, climate and environmental history of Marguerite Bay. The key findings are:

1. The occurrence of a non-erosive glacial regime on Horseshoe Island from 35,780 (38,650–33,380) or 32,910 (34,630–31,370) cal yr BP onwards.
2. The presence of moss fragments embedded within the sediment matrix at 28,830 (29,370–28,320) cal yr BP suggests the earliest onset of deglaciation, or a deglaciation event, on the raised central area on Horseshoe Island immediately post-dating Antarctic Isotopic Maximum 4.
3. The colonisation of the Col 1 site by the fairy shrimp *B. gaini* from 21,110 (21,510–20,730) interpolated cal yr BP. This required the existence of a perennial water body and implies that at least one part of the ice sheet in inner Marguerite Bay was less than 140 m thick (relative to present sea level) at this time. This coincides with, or immediately post-dates Antarctic Isotopic Maximum 2.
4. Robust radiocarbon dated moss macrofossil evidence of Holocene deglaciation at Horseshoe Island from 10,610 (11,000–10,300) cal yr BP during the early Holocene temperature maximum seen in Antarctic ice cores. This was followed by the onset of marine sedimentation in The Narrows, Pourquoi-Pas Island, before 8850 (9260–8480) cal yr BP.
5. A detailed survey of marine relative sea level high stands at 40.79 m (Pourquoi-Pas Island) and 40.55 m (Calmette Bay) sometime after 9000 cal yr BP, suggesting a thicker ice sheet in this region of the Antarctic Peninsula than that recorded elsewhere.
6. The transition from marine sediments to freshwater lake sediments in the Narrows Lake provides a relative sea level constraint of 19.41 m at 7270 (7385–7155) cal yr BP, a mean early Holocene/pre-isolation uplift rate of 12.5 mm yr$^{-1}$, and a mean post-isolation rate of 2.7 mm yr$^{-1}$.
7. Beach clast survey evidence of a period of increased wave energy, likely related to reductions in summer sea-ice extent at Calmette Bay from approximately 8000 yr BP and a dominance of *Chaetoceros* resting spores in The Narrows after 8850 (9260–8480) cal yr BP. This indicates high productivity and stratified surface waters resulting from sea ice melt and coincides with marine geological evidence of a maximum in warm open-ocean and meltwater-related diatoms between c. 9000 and 7000 cal yr BP.
8. Lake sediment evidence of regional warming sometime between 6200 and 2030 cal yr BP which pre-dates the onset of mid- to late-Holocene warming in terrestrial records in the

northern Antarctic Peninsula but ends at a similar time. This is supported by raised beach evidence of open water and increased wave energy in the marine environment c. 6010–5720 to 2300–2010 cal yr BP (Horseshoe Island), and local marine geological evidence (Neny Fjord) of reduced sea ice and productive ocean conditions from c. 7000 to 4000 cal yr BP and increased meltwater discharge from c. 4000 to 2800 cal yr BP.

9. A decline in organic carbon from 2630 to 2030 (Narrows Lake and Col Lake 1 respectively) is interpreted as evidence of the onset of Neoglacial conditions. This corresponds to a return to smaller sub-angular clasts on the Horseshoe Island raised beach after c. 2190–1870 cal yr BP, and is broadly consistent with cooler conditions reported in Neny Fjord from c. 2800 cal yr BP.
10. Diatom and $\delta^{13}C$ vs C/N evidence of a possible increase in the number of birds and seals visiting the catchment of the Narrows Lake after 2100 (2250–2000) cal yr BP, with enhanced nutrient enrichment evident after 1150 (1230–1080) cal yr BP, and particularly from c. 460 (540–380) cal yr BP, the timing of which post-dates the known occupation of the region by penguins, and is broadly consistent with macrofossil evidence of seals (hairs) and penguins (feathers) embedded in local raised beaches.
11. A very recent increase in a diatom species from the genus *Gomphonema* and organic carbon in the top centimetre of the Narrows Lake sediment core after 410 (490–320) cal yr BP, and the renewed onset of sedimentation in the Col Lake 1 sediment core, after c. 400 (490–310) cal yr BP interpreted as a response to the regional late Holocene warming of the Antarctic Peninsula. This is perhaps marginally later than, but still consistent with, the initial onset of late Holocene warming recorded in lake and ice core records from other areas of the Peninsula c. 600–500 years ago, as well as a renewed phase of warming in the local marine geological record sometime after 200 cal yr BP.

## Acknowledgements

This paper contributes to the CACHE-PEP and HOLANT projects led by DH and WV respectively. EV is a post-doctoral research fellow with the Fund for Scientific Research, Flanders. We thank the UK Natural Environment Research Council, British Antarctic Survey and the Belgian Science Policy for research funding, and the British Antarctic Survey and HMS Endurance for logistic support. Additional analyses were carried out at the National Isotope Geosciences Laboratory (NIGL), Keyworth and the NERC Radiocarbon Laboratory, East Kilbride and Beta Analytic. Richard Burt (BAS) provided valuable field assistance and Peter Fretwell (BAS) provided maps and geographical information. Bart Van de Vijver and Ryszard Ochyra provided useful comments on the diatom taxonomy and moss identifications. Julia Wellner and an anonymous reviewer are thanked for their helpful and constructive comments.

## References

Allen, C.S., Oakes-Fretwell, L., Anderson, J.B., Hodgson, D.A., 2010. A record of Holocene glacial and oceanographic variability in Neny Fjord, Antarctic Peninsula. The Holocene 20 (4), 551–564.

Armand, L.K., Crosta, X., Romero, O., Pichon, J.-J., 2005. The biogeography of major diatom taxa in Southern Ocean sediments: 1. Sea ice related species. Palaeogeography, Palaeoclimatology, Palaeoecology 223, 93–126.

Bassett, S.E., Milne, G.A., Bentley, M.J., Huybrechts, P., 2007. Modelling Antarctic sea-level data to explore the possibility of a dominant Antarctic contribution to meltwater pulse IA. Quaternary Science Reviews 26, 2113–2127.

Bennett, K.D., 1996. Determination of the number of zones in a biostratigraphical sequence. New Phytologist 132, 155–170.

Bentley, M.J., Hodgson, D.A., Smith, J.A., Cox, N.J., 2005a. Relative sea level curves for the South Shetland Islands and Marguerite Bay, Antarctic Peninsula. Quaternary Science Reviews 24, 1203–1216.

Bentley, M.J., Hodgson, D.A., Sugden, D.E., Roberts, S.J., Smith, J.A., Leng, M.J., Bryant, C., 2005b. Early Holocene retreat of the George VI Ice Shelf, Antarctic Peninsula. Geology 33 (3), 173–176.

Bentley, M.J., Fogwill, C.J., Kubik, P.W., Sugden, D.E., 2006. Geomorphological evidence and cosmogenic $^{10}Be/^{26}Al$ exposure ages for the Last Glacial Maximum and deglaciation of the Antarctic Peninsula Ice Sheet. Geological Society of America Bulletin 118 (9/10), 1149–1159.

Bentley, M.J., Hodgson, D.A., Smith, J.A., Ó Cofaigh, C., Domack, E.W., Larter, R.D., Roberts, S.J., Brachfeld, S., Leventer, A., Hjort, C., Hillenbrand, C.-D., Evans, J., 2009. Mechanisms of Holocene palaeoenvironmental change in the Antarctic Peninsula region. The Holocene 19 (1), 51–69.

Bentley, M.J., Johnson, J.S., Hodgson, D.A., Dunai, T., Freeman, S., Ó Cofaigh, C., 2011. Rapid deglaciation of Marguerite Bay, western Antarctic Peninsula in the Early Holocene. Quaternary Science Reviews 30, 3338–3349.

Bindschadler, R., Vornberger, P., Fleming, A., Fox, A., Mullins, J., Binnie, D., Paulsen, S.J., Granneman, B., Gorodetzky, D., 2008. The Landsat Image Mosaic of Antarctica. Remote Sensing of Environment 112, 4214–4226.

Blaauw, M., 2010. Methods and code for 'classical' age-modelling of radiocarbon sequences. Quaternary Geochronology 5, 512–518.

Bolmer, S.T., 2008. A note on the development of the bathymetry of the continental margin west of the Antarctic Peninsula from 65° to 71°S and 65° to 78°W. Deep-Sea Research Part II: Topical Studies in Oceanography 55, 271–276.

Bronk Ramsey, C., 2009. Bayesian analysis of radiocarbon dates. Radiocarbon 51 (1), 337–360.

Collins, L.G., Pike, J., Allen, C.S., Hodgson, D.A., 2012. High resolution reconstruction of southwest Atlantic sea-ice and its role in the carbon cycle during marine isotope stages 3 and 2. Palaeoceanography 27, PA3217. http://dx.doi.org/10.1029/2011PA002264.

Cook, A.J., Fox, A.J., Vaughan, D.G., Ferrigno, J.G., 2005. Retreating glacier fronts on the Antarctic Peninsula over the past half-century. Science 308, 541–544.

Cook, A.J., Vaughan, D.G., 2010. Overview of areal changes of the ice shelves on the Antarctic Peninsula over the past 50 years. The Cryosphere 4, 77–98.

Cremer, H., Roberts, D., McMinn, A., Gore, D., Melles, M., 2003. The Holocene diatom flora of marine bays in the Windmill Islands, East Antarctica. Botanica Marina 46, 82–106.

Dean, W.E., 1974. Determination of carbonate and organic matter in calcareous sediments and sedimentary rocks by loss on ignition, comparison with other models. Journal of Sedimentary Petrology 44, 242–248.

Domack, E., Leventer, A., Dunbar, R., Taylor, F., Brachfeld, S., Sjunneskog, C., ODP Leg 178 Scientific Party, 2001. Chronology of the Palmer Deep site, Antarctic Peninsula: a Holocene palaeoenvironmental reference for the circum-Antarctic. The Holocene 11 (1), 1–9.

Domack, E., 2002. A synthesis for site 1098: Palmer Deep. In: Barker, P.F., Camerlenghi, A., Acton, G.D., Ramsay, A.T.S. (Eds.), Proceedings of the Ocean Drilling Program, Scientific Results. Ocean Drilling Program, Texas A&M University, College Station TX 77843–9547, USA.

Emslie, S.D., 2001. Radiocarbon dates from abandoned penguin colonies in the Antarctic Peninsula region. Antarctic Science 13 (3), 289–295.

EPICA, 2006. One-to-one coupling of glacial climate variability in Greenland and Antarctica. Nature 444.

Fretwell, P.T., Hodgson, D.A., Watcham, E., Bentley, M.J., Roberts, S.J., 2010. Holocene isostatic uplift of the South Shetland Islands, Antarctic Peninsula, modelled from raised beaches. Quaternary Science Reviews 29 (15–16), 1880–1893.

Graham, A.G.C., Nitsche, F.O., Larter, R.D., 2011. An improved bathymetry compilation for the Bellingshausen Sea, Antarctica, to inform ice-sheet and ocean models. The Cryosphere 5, 95–106. http://dx.doi.org/10.5194/tc-5-95-2011.

Graham, A.G.C., Smith, J.A., 2012. Palaeoglaciology of the Alexander Island ice cap, western Antarctic Peninsula, reconstructed from marine geophysical and core data. Quaternary Science Reviews 35, 63–81.

Grimm, E.C., 1987. CONISS, a FORTRAN-77 program for stratigraphically constrained cluster analysis by the method of incremental sum of squares. Computers and Geosciences 13, 13–35.

Heroy, D.C., Anderson, J.B., 2005. Ice-sheet extent of the Antarctic Peninsula region during the Last Glacial maximum (LGM) – insights from glacial geomorphology. GSA Bulletin 117 (11/12), 1497–1512.

Heroy, D.C., Anderson, J.B., 2007. Radiocarbon constraints on Antarctic Peninsula Ice Sheet retreat following the Last Glacial Maximum. Quaternary Science Reviews 26, 3286–3297.

Hillenbrand, C.-D., Larter, R., Dowdeswell, J.A., Ehrmann, W., Ó Cofaigh, C., Benetti, S., Graham, A.G.C., Grobe, H., 2010. The sedimentary legacy of a palaeo-ice stream on the shelf of the southern Bellingshausen Sea: clues to West Antarctic glacial history during the Late Quaternary. Quaternary Science Reviews 29 (19–20), 2741–2763.

Hodgson, D.A., Smith, J.A., Burt, R., 2003. Scientific Report – Sledge Bravo 2002–2003. BAS Signals in Antarctica of Past Global Changes: Horseshoe Island, Pourquoi-Pas Island & Calmette Bay British Antarctic Survey (Archives), Cambridge.

Hodgson, D.A., Doran, P.T., Roberts, D., McMinn, A., 2004. Paleolimnological studies from the Antarctic and subantarctic islands. In: Pienitz, R., Douglas, M.S.V., Smol, J.P. (Eds.), Developments in Palaeoenvironmental Research. Long-term Environmental Change in Arctic and Antarctic Lakes. Springer, Dordrecht, pp. 419–474.

Hodgson, D.A., Convey, P., 2005. A 7000-year record of oribatid mite communities on a maritime-Antarctic island: responses to climate change. Arctic Antarctic and Alpine Research 37 (2), 239–245.

Hodgson, D.A., Bentley, M.J., Roberts, S.J., Smith, J.A., Sugden, D.E., Domack, E.W., 2006. Examining Holocene stability of Antarctic Peninsula Ice Shelves. Eos Transactions, American Geophysical Union 87, 305–312.
Hodgson, D.A., Smol, J.P., 2008. High latitude paleolimnology. In: Vincent, W.F., Laybourn-Parry, J. (Eds.), Polar Lakes and Rivers – Limnology of Arctic and Antarctic Aquatic Ecosystems. Oxford University Press, Oxford, UK, pp. 43–64.
Hodgson, D.A., Roberts, S.J., Bentley, M.J., Carmichael, E.L., Smith, J.A., Verleyen, E., Vyverman, W., Geissler, P., Leng, M.J., Sanderson, D.C.W., 2009a. Exploring former subglacial Hodgson Lake. Paper II: Palaeolimnology. Quaternary Science Reviews 28, 2310–2325.
Hodgson, D.A., Roberts, S.J., Bentley, M.J., Smith, J.A., Johnson, J.S., Verleyen, E., Vyverman, W., Hodson, A.J., Leng, M.J., Cziferszky, A., Fox, A.J., Sanderson, D.C.W., 2009b. Exploring former subglacial Hodgson Lake. Paper I: site description, geomorphology and limnology. Quaternary Science Reviews 28, 2295–2309.
Hodgson, D.A., 2011. First synchronous retreat of ice shelves marks a new phase of polar deglaciation. Proceedings of the National Academy of Sciences, USA. http://dx.doi.org/10.1073/pnas.1116515108.
Ingólfsson, Ó., Hjort, C., 2002. Glacial history of the Antarctic Peninsula since the Last Glacial Maximum – a synthesis. Polar Research 21 (2), 227–234.
IPCC, 2007. Climate Change 2007 – the Physical Science Basis Working Group I Contribution to the Fourth Assessment Report of the IPCC Intergovernmental Panel on Climate Change, Cambridge University Press, Cambridge.
Johnson, J.S., Everest, J.D., Leat, P.T., Golledge, N.R., Rood, D.H., Stuart, F.M., 2012. The deglacial history of NW Alexander Island, Antarctica, from surface exposure dating. Quaternary Research 77, 273–280. http://dx.doi.org/10.1016/j.yqres.2011.11.012.
Jones, V.J., Hodgson, D.A., Chepstow-Lusty, A., 2000. Palaeolimnological evidence for marked Holocene environmental changes on Signy Island, Antarctica. The Holocene 10 (1), 43–60.
Juggins, S., 2009. Rioja: Analysis of Quaternary Science Data. http://www.staff.ncl.ac.uk/staff/stephen.juggins/.
Kaiser, J., Lamy, F., Hebbeln, D., 2005. A 70-kyr sea surface temperature record off southern Chile (Ocean Drilling Programme Site 1233). Paleoceanography 20, PA4009. http://dx.doi.org/10.1029/2005PA001146.
Kilfeather, A.A., Ó Cofaigh, C., Lloyd, J.M., Dowdeswell, J.A., Sheng, X., Moreton, S.G., 2011. Ice stream retreat and ice shelf history in Marguerite Trough, Antarctic Peninsula: sedimentological and foraminiferal signatures. Geological Society of America Bulletin 123, 997–1015.
Leventer, A., Domack, E.W., Ishman, S.E., Brachfeld, S., McClennen, C.E., Manley, P., 1996. Productivity cycles of 200-300 years in the Antarctic Peninsula region: understanding linkages among the sun, atmosphere, oceans, sea ice, and biota. Geological Society of America Bulletin 108 (12), 1626–1644.
Livingstone, S.J., Ó Cofaigh, C., Stokes, C.R., Hillenbrand, C.-D., Vieli, A., Jamieson, S.S.R., 2012. Antarctic palaeo-ice streams. Earth-Science Reviews 111, 90–128.
Marshall, G.J., Orr, A., van Lipzig, N.P.M., King, J.C., 2006. The impact of a changing Southern Hemisphere Annular Mode on Antarctic Peninsula summer temperatures. Journal of Climate 19 (20), 5388–5404. http://dx.doi.org/10.1175/JCLI3844.1.
Marshall, G.J., Di Battista, S., Naik, S.S., Thamban, M., 2010. Analysis of a regional change in the sign of the SAM-temperature relationship in Antarctica. Climate Dynamics. http://dx.doi.org/10.1007/s00382-009-0682-9.
Masson-Delmotte, V., Buiron, D., Ekaykin, A., Frezzotti, M., Gallée, H., Jouzel, J., Krinner, G., Landais, A., Motoyama, H., Oerter, H., Pol, K., Pollard, D., Ritz, C., Schlosser, E., Sime, L.C., Sodemann, H., Stenni, B., Uemura, R., Vimeux, F., 2011. A comparison of the present and last interglacial periods in six Antarctic ice cores. Climate of the Past 7, 397–423. http://dx.doi.org/10.5194/cp-7-397-2011.
Matthews, D.W., 1983a. The geology of Pourquoi Pas Island, Northern Marguerite Bay, Graham Land. British Antarctic Survey Bulletin 52, 1–20.
Matthews, D.W., 1983b. The geology of Horseshoe and Lagotellerie Islands, Marguerite Bay, Graham Land. British Antarctic Survey Bulletin 52, 125–154.
McCormac, F., Hogg, A., Blackwell, P., Buck, C., Higham, T., Reimer, P., 2004. Shcal04 Southern Hemisphere Calibration 0–11.0 Cal Kyr BP. Radiocarbon 46, 1087–1092.
Milliken, K.T., Anderson, J.B., Wellner, J.S., Bohaty, S.M., Manley, P.L., 2009. High-resolution Holocene climate record from Maxwell Bay, South Shetland Islands, Antarctica. Geological Society of America Bulletin 121 (11–12), 1711–1725.
Mosley-Thompson, E., Thompson, L.G., 2003. Ice Core Paleoclimate Histories from the Antarctic Peninsula: where do we go from here? In: Domack, E., Leventer, A., Convey, P., Kirby, M. (Eds.), Antarctic Research Series: Historical and Paleoenvironmental Perspectives. Antarctic Research Series, Washington DC, pp. 115–127.
Mulvaney, R., Abram, N.J., Hindmarsh, R.C.A., Arrowsmith, C., Fleet, L., Triest, J., Sime, L.C., Alemany, O., Foord, S., 2012. Recent Antarctic Peninsula warming relative to Holocene climate and ice-shelf history. Nature 489, 141–144.
Ó Cofaigh, C., Dowdeswell, J.A., Allen, C.S., Hiemstra, J.F., Pudsey, C.J., Evans, J., Evans, D.J.A., 2005. Flow dynamics and till genesis associated with a marine-based Antarctic palaeo-ice stream. Quaternary Science Reviews 24, 709–740.
Peltier, W.R., 2004. Global Glacial Isostasy and the Surface of the Ice-Age Earth: the ICE-5G (VM2) model and GRACE. Annual Review of Earth and Planetary Sciences 32, 111–149.
Powers, M., 1953. A new roundness scale for sedimentary particles. Journal of Sedimentary Petrology 23, 117–119.
Quayle, W.C., Peck, L.S., Peat, H., Ellis-Evans, J.C., Harrigan, P.R., 2002. Extreme responses to climate change in Antarctic lakes. Science 295 (5555), 645.
Reimer, P.J., Baillie, M.G.L., Bard, E., Bayliss, A., Beck, J.W., Bertrand, C.J.H., Blackwell, P.G., Buck, C.E., Burr, G.S., Cutler, K.B., Damon, P.E., Edwards, R.L., Fairbanks, R.G., Friedrich, M., Guilderson, T.P., Hogg, A.G., Hughen, K.A., Kromer, B., McCormac, G., Manning, S., Ramsey, C.B., Reimer, R.W., Remmele, S., Southon, J.R., Stuiver, M., Talamo, S., Taylor, F.W., Van Der Plicht, J., Weyhenmeyer, C.E., 2004. Intcal04 terrestrial radiocarbon age calibration, 0–26 cal kyr BP. Radiocarbon 46, 1029–1058.
Reimer, P.J., Baillie, M.G.L., Bard, E., Bayliss, A., Beck, J.W., Blackwell, P.G., Bronk Ramsey, C., Buck, C.E., Burr, G.S., Edwards, R.L., Friedrich, M., Grootes, P.M., Guilderson, T.P., Hajdas, I., Heaton, T.J., Hogg, A.G., Hughen, K.A., Kaiser, K.F., Kromer, B., McCormac, F.G., Manning, S.W., Reimer, R.W., Richards, D.A., Southon, J.R., Talamo, S., Turney, C.S.M., van der Plicht, J., Weyhenmeyer, C.E., 2009. IntCal09 and Marine09 radiocarbon age calibration curves, 0–50,000 years cal BP. Radiocarbon 51, 1111–1150.
Renberg, I., 1990. A procedure for preparing large sets of diatom slides from sediment cores. Journal of Paleolimnology 4, 87–90.
Roberts, S.J., Hodgson, D.A., Bentley, M.J., Smith, J.A., Millar, I., Olive, V., Sugden, D.E., 2008. The Holocene history of George VI Ice Shelf, Antarctic Peninsula from clast-provenance analysis of epishelf lake sediments. Palaeogeography, Palaeoclimatology, Palaeoecology 259, 258–283.
Roberts, S.J., Hodgson, D.A., Bentley, M.J., Sanderson, D.C.W., Milne, G.A., Smith, J.A., Verleyen, E., Balbo, A., 2009. Holocene relative sea-level change and deglaciation on Alexander Island, Antarctic Peninsula, from elevated lake deltas. Geomorphology 112 (1–2), 122–134.
Roberts, S.J., Hodgson, D.A., Sterken, M., Whitehouse, P.L., Verleyen, E., Vyverman, W., Sabbe, K., Balbo, A., Bentley, M.J., Moreton, S.G., 2011. Geological constraints on glacio-isostatic adjustment models of relative sea-level change during deglaciation of Prince Gustav Channel, Antarctic Peninsula. Quaternary Science Reviews 30, 3603–3617.
Round, F.E., Hallsteinsen, H., Paasche, E., 1999. On a previously controversial 'fragilarioid' diatom now placed in a new genus *Nanofrustulum*. Diatom Research 14, 343–356.
Sabbe, K., Verleyen, E., Hodgson, D.A., Vyverman, W., 2003. Benthic diatom flora of freshwater and saline lakes in the Larsemann Hills and Rauer Islands, East Antarctica. Antarctic Science 15, 227–248.
Slota, P.J., Jull, A.J.T., Linick, T.W., Toolin, L.J., 1987. Preparation of small samples for $^{14}C$ accelerator targets by catalytic reduction of CO. Radiocarbon 29, 303–306.
Smith, J.A., Hodgson, D.A., Bentley, M.J., Verleyen, E., Leng, M.J., Roberts, S.J., 2006. Limnology of two Antarctic epishelf lakes and their potential to record periods of ice shelf loss. Journal of Paleolimnology 35, 373–394.
Smith, J.A., Bentley, M.J., Hodgson, D.A., Cook, A.J., 2007a. George VI Ice Shelf: past history, present behaviour and potential mechanisms for future collapse. Antarctic Science 19 (1), 131–142.
Smith, J.A., Bentley, M.J., Hodgson, D.A., Roberts, S.J., Leng, M.J., Lloyd, J.M., Barrett, M.J., Bryant, C., Sugden, D.E., 2007b. Oceanic and atmospheric forcing of early Holocene ice shelf retreat, George VI Ice Shelf, Antarctica Peninsula. Quaternary Science Reviews 26, 500–516.
Smith, J.A., Hillenbrand, C.-D., Kuhn, G., Larter, R., Graham, A.G.C., Ehrmann, W., Moreton, S.G., Forwick, M., 2011. Deglacial history of the West Antarctic Ice Sheet in the western Amundsen Sea Embayment. Quaternary Science Reviews 30 (5–6), 488–505.
Sterken, M., Roberts, S.J., Hodgson, D.A., Vyverman, W., Balbo, A., Sabbe, K., Moreton, S.G., Verleyen, E., 2012. Holocene glacial and climate history of Prince Gustav Channel, northeastern Antarctic Peninsula. Quaternary Science Reviews 31, 93–111.
Taylor, F., Whitehead, J.M., Domack, E., 2001. Holocene paleoclimate change in the Antarctic Peninsula: evidence from the diatom, sedimentary and geochemical record. Marine Micropaleontology 41, 25–43.
Thomas, E.R., Dennis, P.F., Bracegirdle, T.J., Franzke, C., 2009. Ice core evidence of significant 100 year regional warming on the Antarctic Peninsula. Geophysical Research Letters 36, L20704. http://dx.doi.org/10.1029/2009GL040104.
Troels-Smith, J., 1955. Karakterisering av løse jordarter. Danmarks Geologiske Undersøgelse Series IV 3 (10), 1–73.
Turner, J., Arthern, R., Bromwich, D., Marshall, G., Worby, T., Bockheim, J., di Prisco, G., Verde, C., Convey, P., Roscoe, H., Jones, A., Vaughan, D., Woodworth, P., Scambos, T., Cook, A., Lenton, A., Comiso, J., Gugliemin, M., Summerhayes, C., Meredith, M., Naveira-Garabato, A., Chown, S., Stevens, M., Adams, B., Worland, R., Hennion, F., Huiskes, A., Bergstrom, D., Hodgson, D.A., Bindschadler, R., Bargagli, R., Metzl, N., van der Veen, K., Monaghan, A., Speer, K., Rintoul, S., Hellmer, H., Jacobs, S., Heywood, K., Holland, D., Yamanouchi, T., Barbante, C., Bertler, N., Boutron, C., Hong, S., Mayewski, P., Fastook, J., Newsham, K., Robinson, S., Forcarda, J., Trathan, P., Smetacek, V., Gutt, J., Pörtner, H.-O., Peck, L., Gili, J.-M., Wiencke, C., Fahrbach, E., Atkinson, A., Webb, D., Isla, E., Orejas, C., Rossi, S., Shanklin, J., 2009. The instrumental period. In: Turner, J., et al. (Eds.), Antarctic Climate Change and the Environment. Scientific Committee for Antarctic Research, Cambridge, pp. 183–298.
Van de Vijver, B., Frenot, Y., Beyens, L., 2002. Freshwater diatoms from Ile de la Possession (Crozet Archipelago, Subantarctica). In: Bibliotheca Diatomologica, vol. 46. J. Cramer in der Gebrüder Borntraeger Verlagsbuchhandlung, Berlin, Stuttgart, 412 pp.
Van de Vijver, B., Gremmen, N., Smith, V., 2008. Diatom communities from the Sub-Antarctic Prince Edward Islands: diversity and distribution patterns. Polar Biology 31, 795–808.
Vaughan, D.G., Marshall, G., Connolley, W.M., Parkinson, C., Mulvaney, R., Hodgson, D.A., King, J.C., Pudsey, C.J., Turner, J., Wolff, E., 2003. Recent rapid regional climate warming on the Antarctic Peninsula. Climatic Change 60, 243–274.

Verleyen, E., Hodgson, D.A., Vyverman, W., Roberts, D., McMinn, A., Vanhoutte, K., Sabbe, K., 2003. Modelling diatom responses to climate induced fluctuations in the moisture balance in continental Antarctic lakes. Journal of Paleolimnology 30, 195–215.

Verleyen, E., Hodgson, D.A., Sabbe, K., Vanhoutte, K., Vyverman, W., 2004. Coastal oceanographic conditions in the Prydz Bay region (East Antarctica) during the Holocene recorded in an isolation basin. The Holocene 14 (2), 246–257.

Verleyen, E., Hodgson, D.A., Milne, G.A., Sabbe, K., Vyverman, W., 2005. Relative sea level history from the Lambert Glacier region (East Antarctica) and its relation to deglaciation and Holocene glacier re-advance. Quaternary Research 63, 45–52.

Wasell, A., Håkansson, H., 1992. Diatom stratigraphy in a lake on Horseshoe Island, Antarctica: a marine-brackish-fresh water transition with comments on the systematics and ecology of the most common diatoms. Diatom Research 7 (1), 157–194.

Watcham, E.P., Bentley, M.J., Hodgson, D.A., Roberts, S.J., Fretwell, P.T., Lloyd, J.M., Larter, R.D., Whitehouse, P.L., Leng, M.J., Monien, P., Moreton, S.G., 2011. A new relative sea level curve for the South Shetland Islands, Antarctica. Quaternary Science Reviews 30, 3152–3170.

Whitehouse, P.L., Bentley, M.J., Le Brocq, A.M., 2012. A deglacial model for Antarctica: geological constraints and glaciological modelling as a basis for a new model of Antarctic glacial isostatic adjustment. Quaternary Science Reviews 32, 1–24.

Xu, S., Anderson, R., Bryant, C., Cook, G.T., Dougans, A., Freeman, S., Naysmith, P., Schnabel, C., Scott, E.M., 2004. Capabilities of the New SUERC 5MV AMS Facility for $^{14}$C Dating. Radiocarbon 46 (1), 59–64.